DAA/LANGLEY
NCC1-91

Final Report for Work Performed Under Cooperative Agreement NCC1-91

December 1, 1984 - November 1, 1985

IN-61
64847 CR
P 18

Data Inversion Algorithm Development for the Hologen Occultation Experiment

Submitted by:

Larry L. Gordley and Martin G. Mlynczak

College of William and Mary

TABLE OF CONTENTS

page

I Summary 1

II Introduction to HALOE 2

II-1 Experiment Overview 2

III HALOE Instrument Signal 8

IV Fast Broad-Band Method-Application of EGA 14

V Retrieval Scheme 16

VI The LbL Code 20

VI-1 Table Look-up Voigt Function 20

VI-2 LbL Calculation Procedure 24

VII Instrument Characterization Studies 28

VII-1 "Cross-Talk" Effect 28

VII-1.1 Optical Cross-Talk 29

VII-1.2 Electronic Cross-Talk 35

VII-1.2.1 Solar-to-Reference Cross-Talk 35

VII-2 Balance Offset Effects 38

VII-3 Correction Formula Interdependence 41

VIII Detector to Beam Non-uniformity Studies 45

IX Consultation Services 50

IX-1 HALOE Instrument Testing Service 50

IX-2 Algorithm Development Consultation 51

X Conclusion 52

APPENDIX A 53

APPENDIX B 56

APPENDIX C 65

APPENDIX D 71

I. Summary

The following report is a description of activities performed and results obtained over the past year 12/84-12/85 by The College of William and Mary under cooperative agreement (NCC1-91).

This grant was awarded primarily for developing an adequate technique to reduce the Halogen Occultation Experiment (HALOE) data set. The HALOE experiment will begin shortly after launch of the Upper Atmosphere Research Satellite (UARS) in late 1989.

The successful retrieval of atmospheric parameters from radiometric measurement requires not only the ability to do ideal radiometric calculations, but also a detailed understanding of instrument characteristics. Therefore a considerable amount of time was spent participating in instrument characterization in the form of test data analysis and mathematical formulation.

Both electrical and optical characterization are important for accurate signal processing. Analyses of solar-to-reference interference (electrical cross-talk), detector non-uniformity, instrument balance error, electronic filter time-constants and noise character were conducted. Optical studies included, beam uniformity analyses, interference between gas-and-vacuum paths (spectral cross talk) and in-orbit signal estimates. Consulting roles were played during tests that included field-of-view measurements, gas cell response, spectral filter measurements, and signal drift measurements to name a few. A second area of effort was the development of techniques for the ideal radiometric calculations required for HALOE data reduction. The computer code for these calculations must be extremely complex and fast. During the year, a scheme for meeting these requirements was defined and the algorithms needed for implementation are currently under development. Most of the work in this area has been in the development of a new transmittance code. When completed, "exact" (commonly referred to as "line-by-line" or "LbL") limb path transmission profiles will be possible in one program execution at previously unattainable speeds.

In addition, the formulation for a less accurate, faster radiance calculation method has been defined. This method will be combined with the "LBL" method in the overall retrieval scheme.

A third area of work included consulting on the implementation of the EGA (emissivity growth approximation) method of absorption calculation into a HALOE broad band radiometer channel retrieval algorithm.

Most of these areas of work will be detailed in the following report.

II. Introduction to HALOE

II-1 Experiment Overview

The bulk of this section has been taken directly from the HALOE software release I document. It is included here only for the unfamiliar reader.

The Halogen Occultation Experiment (HALOE) is a satellite solar occultation experiment being developed as part of the Upper Atmosphere Research Satellite (UARS) program. The objective of UARS is to study the physical processes acting within and upon the stratosphere, mesosphere, and lower thermosphere of the Earth. A central factor in meeting this objective is the development and launch of a free-flying scientific observatory to provide needed measurements. Scheduled for launch in 1989, this UARS observatory will have a complement of 11 scientific instruments and will operate at an altitude of 600 km and an orbital inclination of 57 degrees. As part of this instrument complement, HALOE will provide measurements of key species in the ClO_x, NO_x, and HO_x chemical cycles (i.e. O_3. HCl, HF, NO, NO_2, CH_4, and H_2O), and the HALOE team will provide scientific studies with these and related data.

The HALOE experiment is based on the concept of measuring the absorption of solar radiation by atmospheric constituents along a limb-viewing path during sunrise and sunset (i.e. occultation) events (Fig. 1). Vertical scans of the upper atmosphere are obtained by tracking the solar disk during an occultation. From these vertical absorption scans, associated atmospheric temperature data, and orbital information, species concentration profiles as a function of pressure (and altitude) can be inferred. This solar occulation technique offers the advantages of high sensitivity due to long absorbing paths, high vertical resolution due to weighting of the absorption near the ray tangent altitude (H_0 in Fig. 1), and a strong relatively constant intensity radiation source in the sun.

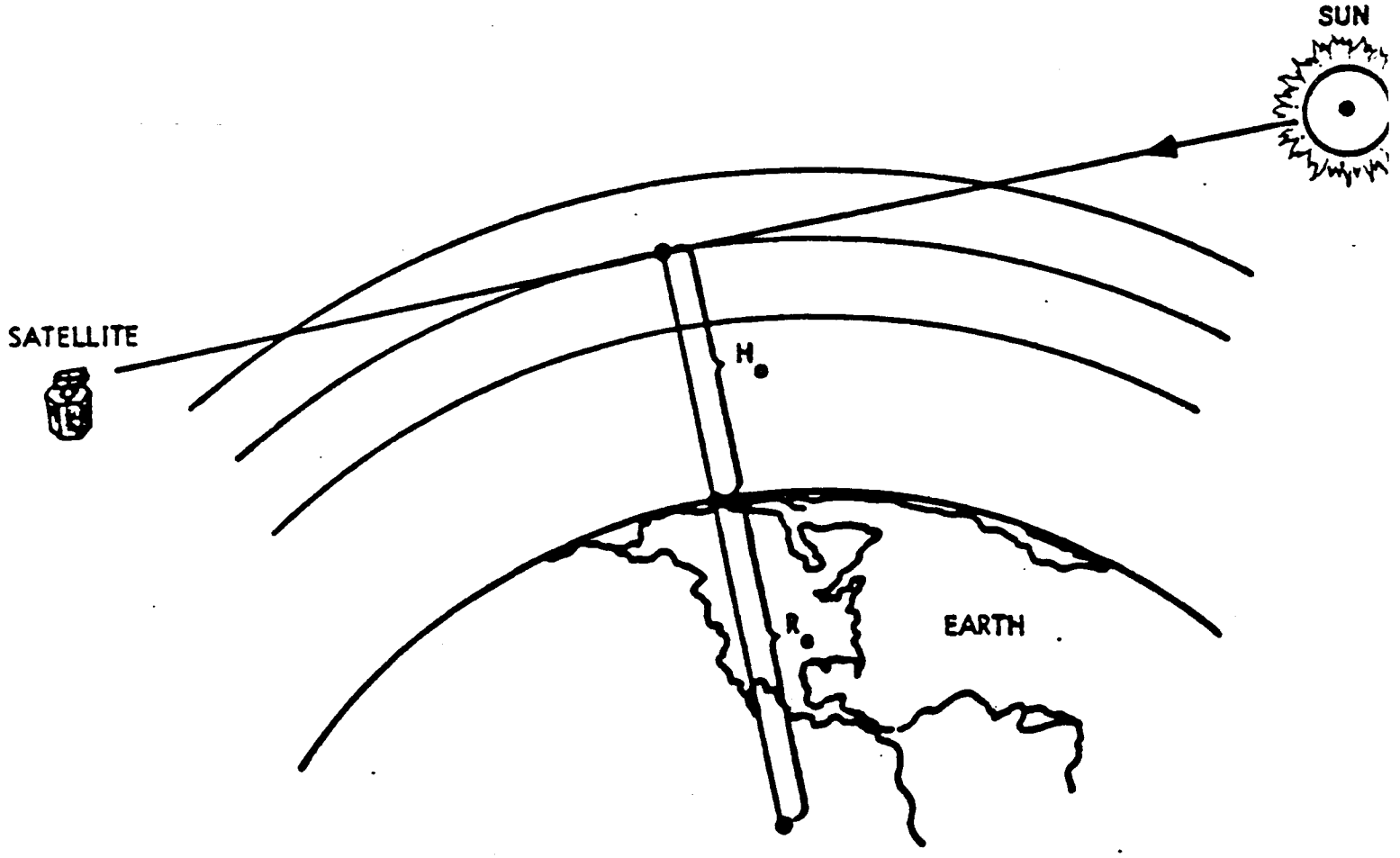

FIG. 1 EXPERIMENT GEOMETRY

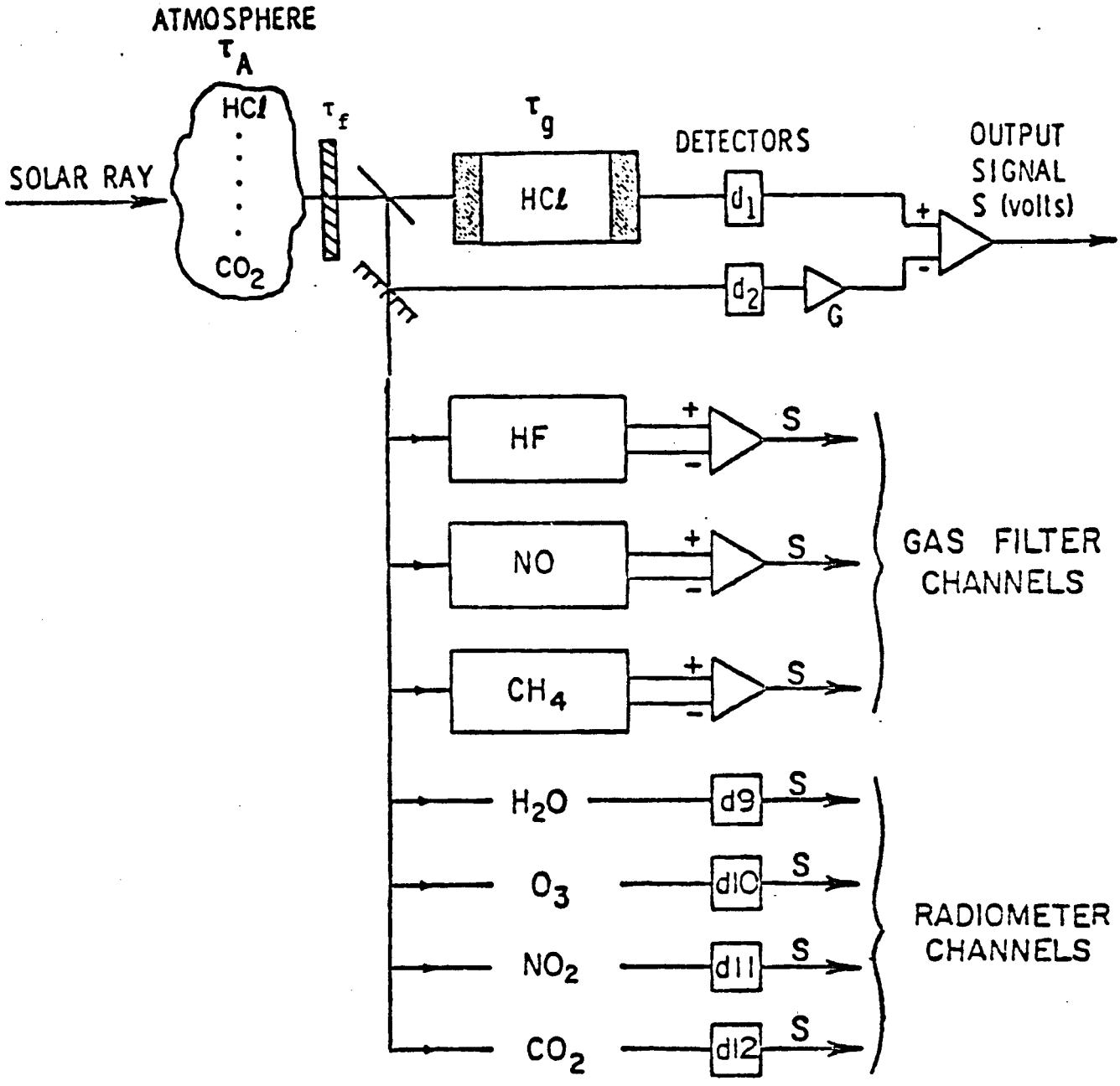

FIG. 2 HALOE INSTRUMENT TECHNIQUE

As illustrated in Fig. 2, the HALOE instrument uses gas filter correlation radiometry for measurements of HCl, HF, CH_4, and NO and uses broadband filter radiometry for measurement of tangent point pressure (from CO_2 absorption), O_3, H_2O, and NO_2. The gas filter correlation concept is based on correlation between the spectral content of the solar radiation passing through the atmosphere and that introduced by a gas cell containing the species of interest. It provides the high effective spectral resolution needed for isolating spectral signatures of a target gas from the effects of interfering absorbers. The broadband filter radiometer concept is similar to that used successfully on the Nimbus satellites.

The HALOE instrument provides four types of operations during the science data portion of an occultation event: balance, solar scan, calibration, and atmospheric data collection. The first three operations occur while HALOE is viewing the sun above the atmosphere. In the balance operation, electronic gain adjustments are made to match, to some offset, the signals from the two separate paths in each gas correlation channel. The solar scan mode provides five complete scans (down and back) of the sun to characterize the solar relative intensity curve. In the calibration operation, a calibration wheel containing gas cells for the four gas filter target gases and a series of neutral density filters are cycled through the optical path. This provides a check on gas response, radiometric calibration, and instrument balance. Finally, in the atmospheric data collection operation, HALOE tracks the sun through the atmosphere to obtain modulation (gas correlation channels) and radiance (radiometer channels) profiles. For a sunset event, all four operations are included; for a sunrise event, the balance is omitted.

In effect the HALOE technique attempts to differentiate between the absorption of the gas of interest and the total broad band absorption, which can be as small as one part in 100. This one part in 100 then is desired to be known to at least 10% accuracy, requiring knowledge to .1% of the total adsorption. Since the HALOE signal

is proportional to transmission (where transmission = 1-absorption) and transmission is typically >.9, the total signal must be measured with a precision of .01% or better. As can be seen by the above description, the measurement is done by the differencing of two large signals. This implies that the consistency of these two large signals must be maintained by the instrument and estimated by calculations to better than .01%. This accuracy can be obtained only by careful characterization of the instrument and high resolution calculations of the spectral correlation between atmospheric and gas cell absorption features.

Both of these general tasks have been addressed over the previous year.

III. HALOE Instrument Signal

As discussed above, the success of HALOE will depend on how well the signal can be modeled. Therefore considerable effort was given to putting the HALOE signal equation into a form that would produce insight and understanding. This would allow test results to be interpreted with more confidence, instrument specifications to be better evaluated if necessary, and possible ideas to surface on the best attack of the retrieval problem.

HALOE attempts to produce a signal that is highly correlated with the atmospheric absorption of a specific gas. This is done by effectively differencing two occultation radiometer measurements. The input for one optical path measurement has spectral radiation, in regions of the specified gas absorption, removed by passing the input through a gas cell. The idea is that the two measurements will be similar, except for sensitivity to atmospheric absorption by the type of gas in the cell.

The study of this concept prompted a few questions. 1. Can the signal ΔV (commonly referred to as modulation) be formulated in a way analogous to a radiometer? 2. If not, what is the difference? 3. Will a change in formulation allow radiometer techniques to be applied to the HALOE retrieval problem?

The HALOE modulation equation is:

$$\Delta V = \int_{\nu_1}^{\nu_2} S f \tau_a \tau_c (G \tau_g \tau_1 - \tau_2) d\nu \qquad (1)$$

where S = source function (includes normalization (or conversion constant))

G = gain factor necessary for balance

f = broad spectal filter function

Δv = voltage

τ_a = atmospheric transmission

τ_c = instrument response common to both vacuum and gas path

τ_1 = instrument response unique to gas path

τ_2 = instrument response unique to vacuum path

All variables are a function of ν (wavenumber) except G which is constant. Also $\nu_2 > \nu_1$ and $f(\nu) = 0$ for $\nu < \nu_1$ and $\nu > \nu_2$. The integral will be assumed over the non-zero range of $f(\nu)$.

The instrument is balanced under conditions of $\tau_a = 1$, or

$$\Delta V_B = \int Sf'(G'\tau_g - 1)d\nu \tag{2}$$

where $$G' = G\tau_1/\tau_2 \tag{3}$$

$$f' = f\tau_c\tau_2 \quad \text{(Vacuum path instrument spectral response)} \tag{4}$$

One can show that (see appendix A)

$$\Delta V \simeq \underbrace{\Delta V_B}_{\text{Term 1}} - \underbrace{(\overline{G} - 1)(V_{V0} - V_{VI})}_{\text{Term 2}} + \underbrace{\overline{G} \int Sf'\xi_a\xi_g d\nu}_{\text{Term 3}} \tag{5}$$

where V_{V0} = vacuum path signal viewing above the atmosphere

V_{VI} = vacuum path signal viewing through atmosphere

$\xi_a = 1 - \tau_a$

$\xi_g = 1 - \tau_g$

$\overline{G} = 1/\overline{\tau}_g$

$\overline{\tau}_g = \int Sf'\,\tau_g d\nu / \int Sf'd\nu$

Term 1 is set to zero at balance, leaving only terms 2 and 3. Term 2 is proportional to minus the average broad band absorption while term 3 is proportional to the average absorption over the effective gas filter, $f'\xi_g$ (see Appendix A). It is interesting to note the broad band absorption term goes to zero for $\overline{G} = 1$. This could have been achieved by balancing the instrument with an empty cell in place then switching to a filled cell for recording data. This would have allowed the luxury of spectral calculations being necessary only where ξ_g is significantly non-zero.

However, the advantage of the HALOE balance is that absorption sources with zero correlation to ξ_g will balance to zero (i.e. wide filter and gas filter average absorption are equal). The effects of poorly known continuum or randomly distributed spectral features are minimized by the HALOE balance.

Our first two questions are now answered. Term 2 and term 3 of equation 5 are analogous to simple radiometers. As we will see in the next section, term 2 is equivalent to two radiometers with slightly different broad band filters (G'f & f'). Term 3 of equation 5 is formulated identically to an emission radiometer where the filter is $G'f\xi_g$ and the Plank function is replaced by S, the solar source function. However, the third question is still in doubt. Although the formulation is adequate, the broad band filter calculation techniques may not be capable of modeling term 3 adequately.

To gain more insight into the ΔV signal, the various components of equation 5 were evaluated for each of the HALOE gas filter channels using a model atmosphere. The calculations were performed for six paths with tangent altitudes of 62, 50, 40, 30, 20, and 10 kilometers. The computations were simplified by colapsing the optical mass into the tangent layer, so the calculations are intended only for a rough study of relative magnitudes. The mixing ratio profiles used, are in Table 1. The results of the calculations appear in Tables 2a, 2b, 2c and 2d. As can be seen, the terms of equation 5 have been normalized by V_{VO} then divided by 2×10^{-5}. This puts them into instrument noise level units which are roughly $2 \times 10^{-5}\ V_{VO}$. The only column in the tables that needs explanation is the last. This is an attempt to estimate the signal change in V_{VI} if the principle absorber (the gas of interest) were removed from the atmosphere. That is V'_{VI} is the evaluation of V_{VI} excluding the gas of interest. Therefore, the last column represents the largest possible signal due to the gas of interest.

If the interferring absorbers have zero correlation with the gas filter, with little overlap of spectral lines, one would expect column 2 and 6 to be nearly equal. If there were very little spectral absoption by interferring gases in regions of gas filter absorption, then one would expect columns 4 and 6 to be nearly equal. By inspecting Table 2a-2d we see that one or both conditions may exist above 30 km, but below 30 km there is significant non-zero correlation and/or spectral line overlap. This implies that retrieval calculations will need to incorporate detailed characterization of line shape at the lower altitudes, especially when Doppler shift effects are included. To handle these effects with broad band techniques, large empirical adjustments will be necessary and/or a large increase in precalculated data tables along with increased complexity in the table utilization algorithms.

Mixing Ratio Profiles Used in Simulations

TABLE I

Mixing Ratio P_{gas}/P_{air}

ALT (km)	HF	HCl	CH_4	NO	H_2O	N_2O	O_3	NO_2
62	2.9E-10	1.3E-9	8.0E-9	3.0E-9	3.0E-6	1.7E-11	0.96E-6	1.0E-10
50	4.5E-10	1.3E-9	1.0E-7	1.0E-8	5.0E-6	3.1E-6	3.1 E-6	1.0E-9
40	4.0E-10	1.5E-9	4.0E-7	1.2E-8	4.6E-6	1.6E-8	7.3 E-6	3.5E-9
30	3.0E-10	1.0E-9	8.0E-7	2.5E-9	4.8E-6	9.0E-8	6.6E-6	7.5E-9
20	6.0E-11	5.0E-10	1.3E-6	2.5E-10	4.4E-6	2.4E-7	2.6E-6	9.0E-10
10	6.0E-13	2.4E-11	1.6E-6	3.0E-10	4.0E-5	3.2E-7	1.3E-7	3.0E-10

TABLE 2a

HF Channel

Tangent Ht. km	ΔV	Term 2 (Eq. 5)	Term 3 (Eq. 5)	$V_{VO}-V_{VI}$	$V^{i}_{VI}-V_{VI}$
62	.11	-.23	.34	2.27	.16
50	.72	-2.07	2.79	21.44	1.18
40	3.39	-6.27	9.66	62.00	4.52
30	11.95	-16.61	28.58	164.10	13.42
20	23.45	-51.08	74.53	504.60	25.50
10	35.23	-441.69	476.92	4362.90	12.60

(units of 2×10^{-5} V_{VO}) $\overline{G} = 1.1012$

TABLE 2b

HCl Channel

Tangent Ht. km	ΔV	Term 2 (Eq. 5)	Term 3 (Eq. 5)	$V_{VO}-V_{VI}$	$V^{i}_{VI}-V_{VI}$
62	.52	-.02	.53	.84	.52
50	2.26	-.17	2.43	9.11	2.33
40	8.74	-1.64	10.38	88.23	9.43
30	28.45	-12.15	40.60	653.80	33.61
20	43.40	-75.72	119.13	4073.72	81.69
10	-45.65	-438.55	393.89	23592.86	63.40

(units of 2×10^{-5} V_{VO}) $\overline{G} = 1.0186$

TABLE 2c

NO Channel

Tangent Ht. km	ΔV	Term 2 (Eq. 5)	Term 3 (Eq. 5)	$V_{VO}-V_{VI}$	$V^{i}_{VI}-V_{VI}$
62	.05	-1.72	1.77	41.32	1.41
50	16.17	-7.65	23.83	183.00	21.61
40	84.61	-18.33	102.94	438.30	90.78
30	164.27	-49.25	213.52	1177.50	200.00
20	94.96	-176.38	271.34	4217.04	210.76
10	42.17	-948.01	990.18	22665.87	247.66

(units of 2×10^{-5} V_{VO}) $\overline{G} = 1.1418$

TABLE 2d

CH_4 Channel

Tangent Ht. km	ΔV	Term 2 (Eq. 5)	Term 3 (Eq. 5)	$V_{VO}-V_{VI}$	$V^{i}_{VI}-V_{VI}$
62	.27	-.25	.52	.48	.22
50	14.53	-10.06	24.59	19.09	17.00
40	201.68	-143.96	345.65	273.19	251.13
30	815.02	-732.17	1547.18	1389.27	1191.21
20	2921.96	-2915.51	5837.47	5532.08	5193.62
10	6775.10	-11749.35	18524.45	22293.99	21596.13

(units of 2×10^{-5} V_{VO}) $\overline{G} = 1.5270$

IV. Fast Broad-Band Method - Application of EGA (Emissivity Growth Approximation) to HALOE

Limb geometry remote sensing experiments have the ability to infer unique mixing ratio profiles from measured radiance proviles over significant vertical altitude ranges, at least to the vertical resolution of the instrument. This vertical resolution is determined by vertical field-of-view, sample spacing and noise. For HALOE, it should be about 2 km throughout the stratosphere. Because of the extremely non-linear nature of the radiative transfer equation, accurate solutions are obtained only through iterative procedures involving many successive calculations of the forward problem. (This inverse problem can be solved in a closed form only if linearized about an atmospheric state assumed "close" to the true solution. This necessitates an a prior knowledge and/or assumption about the true state, giving unreliable results. (The method is unaccepatable in our opinion.) The ability to do many fast and accurate forward calculations becomes the key to credible inversion of the measured radiance profiles.

The most successful method, to date, for doing the broad band forward calculation has been the EGA. This method was applied to the LIMS (Limb Infrared Monitor of the Stratosphere) experiment operational data processing with excellent results. We are now in the process of applying the technique to the HALOE modulation calculation.

Very simply stated, the EGA method calculates broad-band absorption or emission over inhomogeneous paths using tables consisting of broad-band emissivities, $\overline{E}(U,T,P)$, for homogeneous paths. These homogeneous emissivities represent a wide range of mass path "U", temperature "T" and pressure "P" values. The broad-band emissivity is defined as:

$$\bar{E}(U,T,P) = \int_{\nu_1}^{\nu_2} F(\nu)B(\nu,T)\xi(U,T,P,\nu)d\nu / \int_{\nu_2}^{\nu_2} F(\nu)B(\nu,T)d\nu \qquad (6)$$

where F = Broad-band spectral filter

B = Plank function

ξ = Monochromatic absorption

ν = wavenumber

F = 0 outside of range ν_1 to ν_2

The use of these tables is described in Gordley and Russell, 1981.

Equation 6 describes the tables that would be used for an emission calculation. For absorption calculations, as for HALOE, the Planck function $B(\nu,T)$ is replaced with the solar source function $B(\nu,6000°K)$. The same forward emission calculation procedures can then be used to calculation absorbed solar radiance.

From equation A4 of appendix A we see that

$$\Delta V = \int Sf'\xi_a d\nu - \int Sf'G'\xi_a d\nu + \int Sf'G'\xi_g\xi_a d\nu \qquad (7)$$

(where ΔV_B is assumed balanced to 0). This is the equivalent of measuring absorption using three separate radiometer channels with filters F_1, F_2 and F_3 where

$$F_1 = F\tau_C\tau_2$$

$$F_2 = Gf\tau_C\tau_1$$

$$F_3 = Gf\tau_C\tau_1\xi_g$$

The development of the algorithm to use the EGA techniques in evaluting equation 7 is underway with a preliminary functional code likely to be complete by early 1986.

V. Retrieval Scheme

As already dicussed, the accurate modeling of the HALOE signal must include effects that originate from the sharp spectral features in both the gas cell and atmospheric spectra. When the relative spectral position or shapes of these features change due to Doppler shifting, pressure broadening, etc., the ΔV signal can incure large relative changes. The ability to include these effects in an EGA algorithm with consistent and sufficient accuracy over all atmospheric and measurement scenarios is not only unlikely but difficult to validate. Only exact LbL calculations appear to be adequate for this requirement, but their use in interative retrievals is prohibitively expensive and time consuming.

We have developed a scheme that will combine the accuracy of the LbL method and the speed of the EGA method while circumventing their respective disadvantages of time and inaccuracy.

Figure 3 displays the retrieval procedure in flow diagram form. The following reasoning is the source of this scheme.

The EGA forward calculations are fast and precise and will be used in the calculation intensive iterative retrieval algorithm. However, it is assumed that given the correct atmospheric state, the signal levels calculated by the EGA will be in error. This error, in our experience, is typically a systematic function of pressure and masspath. Therefore, given some measured signal as input, the EGA algorithm will relax to an incorrect solution. The LbL algorithm can be used to spot-check the EGA error at several target altitudes by using the EGA solution as input to an LbL forward calculation of signal. The difference between the measured signal and the LbL estimated signal is then used to infer a needed adjustment of the signal profile that was input to the EGA retrieval program. Stated another way, an adjustment is made to the measured signal that effects the correct retrieved solution. This adjustment is infered and continually refined by periodic and/or sparse LbL calcuations.

$Q(Z)$ = Mixing Ratio

$M(Z)$ = Measured Moduation

$M_e(Z)$ = Adjusted Modulation

$M_L(Z)$ = Calculated Modulation

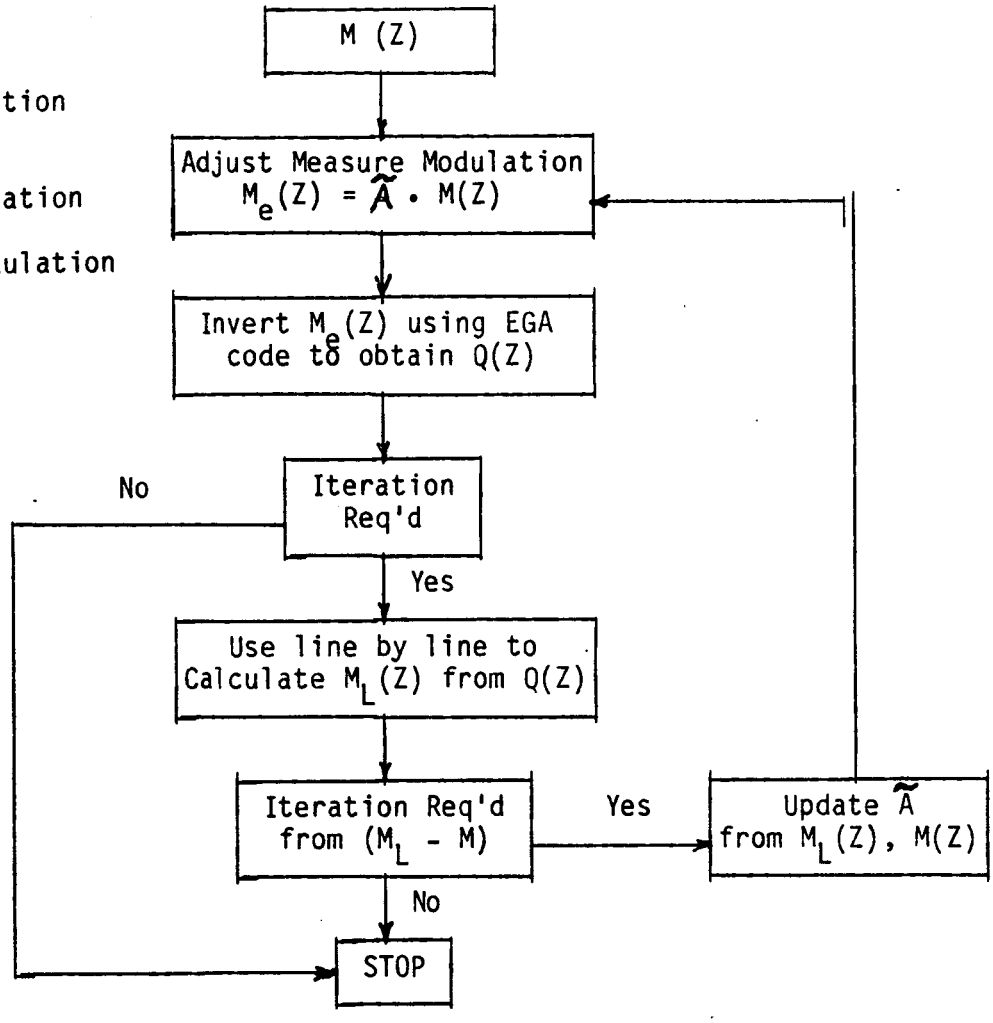

Figure 3.- Modulation inversion procedure

The measurement adjustment concept may at first seem non-rigorous and unsettling. However, viewed from another perspective, it is in reality in LbL retrieval in which an EGA code is used as a very sophisticated relaxation and interpolation scheme. To see this, let's look at a likely procedure in determining and maintaining an adjustment function "A".

The problem is to find an adjustment "A" which we'll assume is a function of tangent pressure P.

$$M_e = A(P)M_m(P) \tag{8}$$

where M_m = the measured modulation

M_e = the modulation that, when input to an EGA code will effect the correct retrieval

Initially we will assume A = 1, retrieve a mixing ratio, then use the mixing ratio as input for an LbL calculation of modulation $M_L(P)$. If the EGA calculations are reasonably accurate with systematic errors, one might assume that a change of $\Delta M_e(P)$ will effect a change $\Delta M_L(P)$ with the following relationship.

$$\frac{\Delta M_e(P)}{M_e(P)} = \frac{\Delta M_L(P)}{M_L(P)} \tag{9}$$

Using equations 8 and 9 one can show that:

$$A(P) = \frac{M_e(P)}{M_L(P)}$$

A starting scenario may be as follows:

1. Set $A(P) = 1$ and $A^L(P) = 0$
2. Retrieve a mixing ratio $Q(P)$ using $M_e(P) = A(P)M_m(P)$
3. Stop if $|A(P)-A^L(P)| < \varepsilon$ (ε = convergence criterion)
4. Set $A^L(P) = A(P)$
5. Use $Q(P)$ for LbL calculation of $M_L(P)$
6. Set $A(P) = M_e(P)/M_L(P)$ and go to step 2.

The above sequence could involve many LbL executions, depending on relaxation rates. However, on subsequent retrievals, the initial adjustment would be done with the previously estimated A(P). LbL calculations could be limited by doing only a small number of tangent pressures. The update of A(P) at these few pressures could be used to infer the other levels through an interpolation or fitting procedure. It may be found that even these sparse update calculatons need not be performed every orbit since occulation tangent latitudes very slowly with time. There are many possibilities for holding LbL calculation to a minimum while maintaining retrieval integrity. The most important aspect of the method is that line-by-line signal simulations, using retrieval mixing ratios, are required to match measured signals. This is the equivalent of a line-by-line retrieval.

VI. The LbL Code

It should be clear from the previous section that the quality of the modulation retrieval results will be strongly dependent on the efficiency of the LbL code. Speed, flexibility and accuracy are the required ingredients for an adequate LbL algorithm. In view of these requirements, a significant effort was made in designing and developing a new Lbl code for this specific application. The goal was to develop a code with the following characteristics:

a) Efficient table look-up Voigt function.

b) No input/output of cross-sections.

c) Complete limb signal profile.

d) Cross-section calculations independent of number of tangent paths.

Ninety percent of the time and expense of currently available LbL codes can be traced to the calculations of the Voigt function and the reading and writing of calculated cross section values. Therefore these operations must be accelerated or reduced in number before a faster code can be realized.

VI. - 1 Table Look-Up Voigt Function

The Voigt function can be viewed as the convolution of two separate symmetric functions about a center frequency. These two funtions are a Doppler broadening function and a Lorentz (pressure) broadening function. The first is a Gaussion and the second takes the form of:

$$C\alpha/[(\nu-\nu_0)^2 + \alpha^2]$$

where c is a constant equal to $1/\pi$, α is the transition halfwidth at STP (standard temperature and pressure) and $(\nu - \nu_0)$ is the wavenumber distance from transition center ν_0. ν, ν_0 and α are in units of cm^{-1}.

The halfwidths of there two functions derive from two different physical phenomena. The Doppler is due to the distribution of molecular kinetic motion causing various doppler shifts of the transition. The Lorentz is due to collisional warping of the quantum states causing a change in energy levels. The Doppler broadening is therefore temperature dependent while the Lorentz broadening is, to first order, density dependent. The range of temperature/density combinations in the atmosphere can be extreme, requiring careful planning and validation of any table look-up scheme used for the Voigt function evaluation. In addition, the behavior of the Doppler and Lorentz broadening functions in the "wings" (large distance in wavenumbers from line center) is quite different, $\exp[-(\nu_0 - \nu)^2]$ versus a $1/(\nu_0 - \nu)^2$ type behavior. Therefore, the Lorentz function will always dominate at large distances from line center.

The primary objective was to develop a code that would evaluate the Voigt function as quickly as possible with at least the minimum accuracy required. The goal for minimum accuracy was set at 1% relative accuracy for points on the Voigt curve with .1% integrated accuracy. These were met with the scheme described below.

Normally the Voigt function is expressed as a function of two parameters x and y.

$$x = |\nu - \nu_0| / \alpha_D$$

$$y = \alpha_L / \alpha_D$$

α_L = Lorentz halfwidth

α_D = Doppler halfwidth

If the table look-up is to be fast, the scheme must allow linear interpolation over subsets of the tables. The logic to find the proper subset must be fast, implying few subsets. It was found that the variation of the function over the x, y plane made it difficult to choose table subsets that accommodated easy look-up interpolations. Therefore a different mapping formulation was used in which the independnt parameters were defined as,

$$x' = |\nu - \nu_o|/(\alpha_L + \alpha_D)$$

$$y' = \alpha_L/\alpha_D$$

Note: $y' = y$

$x' = x/(y + 1)$.

With this transformation of independent variables, it was found that the domain of x' and y' could be partitioned into 4 regions, as described in Table 3.

In the first region a simple Lorentz function calculation is performed. It was found that the evaluation of the Lorentz function was faster than table look-up logic for extended x' regions. In addition, this allows for distant Lorentz wings. The last 3 regions are done using table look-up and linear interpolation between adjacent x' and y' values. Figure 4 is a contour of percent error over the domain of x' and y'.

TABLE 3
TVOIGT Routine Table
Partitioning

	X'		Y'	
	Limits	Spacing	Limits	Spacing
Region 1	$X' \geq X_B$	N/A	Unlimited	N/A
Region 2	$X' < X_B$	.1	$5 < Y' \leq 11$	.5
Region 3	$X' < X_B$	.1	$.1 < Y' \leq 5$	.1
Region 4	$X' < X_B$	.1	$0 < Y' \leq .1$	.002
	$X_B = (11.0 - Y)/(0.6875(Y + 1))$			

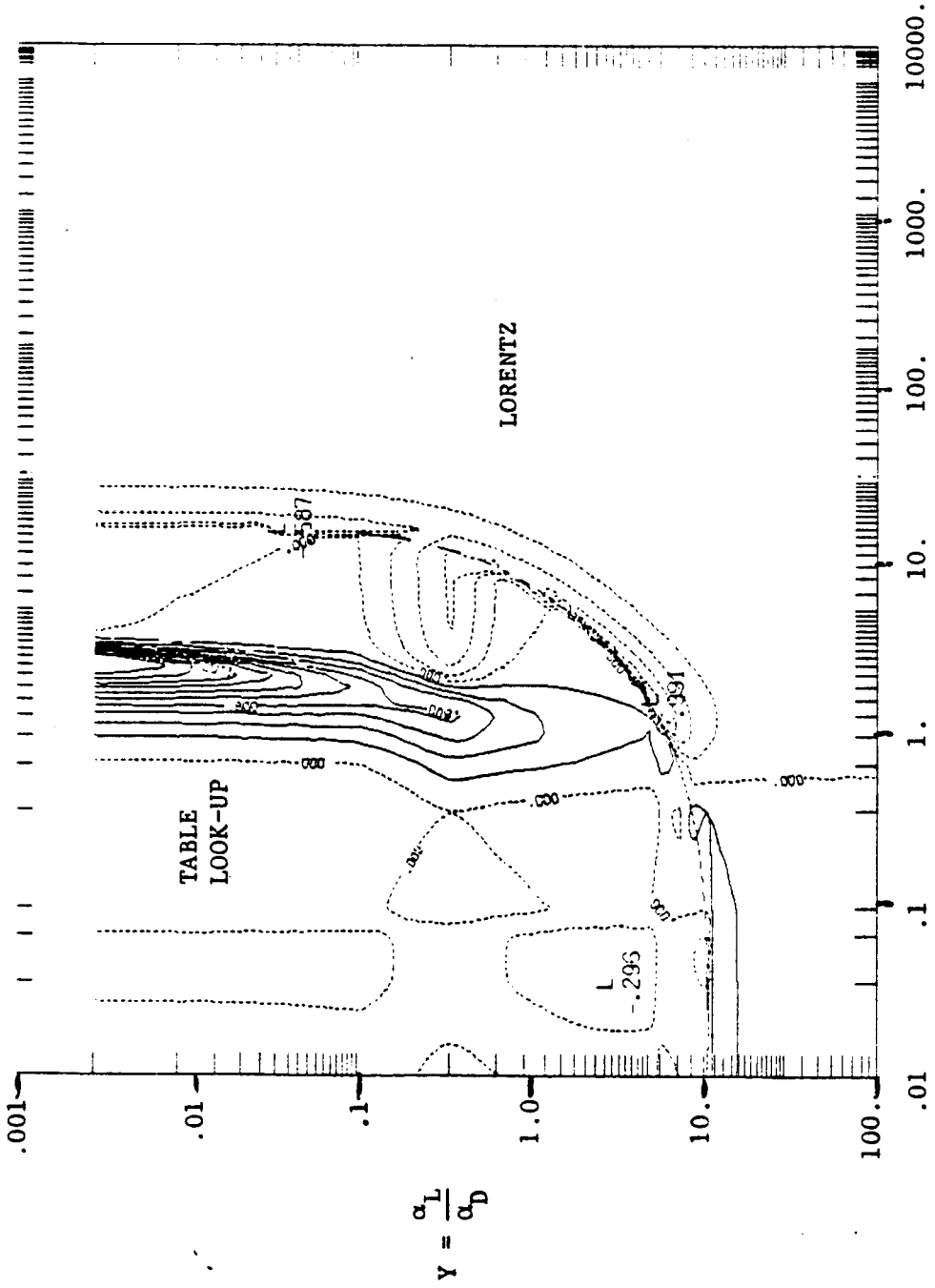

Figure 4 Voigt Error %

VI.-2 L-b-L Calculation Procedure

Reducing L-b-L calculation time requires minimizing cross section calculations and input/output operations. To achieve this goal with the additional requirement that transmission for multiple paths be calculated with a minimum of computational overhead, we have ordered and separated the necessary operations in a unique fashion.

First, the integration over spectral frequency is done as the outside loop. That is, all computations involving cross sections over an interval $\Delta\nu$ are completed before proceeding to the next spectral interval. This avoids the necessity of writing cross-section values to disk or storing large numbers of cross-section values for later use.

Second, the spectral calculations are kept to a minimum by calculating cross-sections at pressure and temperature conditions associated with various attitudes of the atmosphere being analyzed. It is then assumed that the integrated transmission can be modeled sufficiently for each tangent path by a combination of these P, T conditions and an associated optical mass. A separate code, given temperature, pressure and mixing ratio profiles and tangent ray altitudes, will determine the needed P, T conditions for cross-section calculations and a corresponding optical mass array for each ray path. Therefore, if the L-b-L program recieves N comibinations of (P, T) for cross-section calculation and there are M ray paths to be modeled, it will recieve an MXN array of optical mass values, for each absorbing gas.

Figure 5 shows a pseudo FORTRAN code used to descibe the order of calculation. Figure 6 graphically depicts the possible relation between levels selected for temperature/pressure conditions (TPC's) and the mass integration along the tangent ray. The masspath is integrated along the ray in finite elements determined by the dashed curve borders. The mass of each element is partitioned into the two nearest

TPC's. The partitioning is done by a Lorentz half width weighting scheme. For instance if T_1, P_1 and T_2, P_2 are the temperature and pressures of TPC levels 1 and 2, then the mass U_e is partitioned as follows:

$$U_1 = U_e[\alpha_2 - \alpha_e]/[\alpha_2 - \alpha_1]$$

$$U_2 = U_e - U_1$$

where

$$\alpha_1 = \alpha_{io} \frac{P_i}{P_o}[T_o/T_i]^\gamma$$

α_{io} = halfwidth at standard pressure and 296 K.

γ = a gas dependent constant typically $.5<\gamma<1$.

T_o, P_o = standard temperature and pressure.

It is obvious that the ray transmission error should approach zero as the TPC's become more numerous and closely spaced. This implies that there should be a spacing that gives the maximum error that can be tolerated. Studies are planned for determing this spacing. Also note that to achieve this desired accuracy at a few selected tangent levels, the optimum TPC spacing will likely be nonuniform.

The code for performing all of these L-b-L calculations is in the final stage of development and a prototype should be operational by 3/86.

```
        Initialize Arrays
      DO 90 n = 1, N
      DO 50 i = 1, I
      DO 40 k = 1, K
        Calculate J cross-section for
        Segment n, SCBi, gask--C(j)
      DO 30 m = 1, L
      DO 20 j = 1, J
        A(j,m) = A(j,1) - u(m,i,k)*C(j)
   20 CONTINUE
   30 CONTINUE
   40 CONTINUE
   50 CONTINUE
      DO 70 m = 1, L
      DO 60 j = 1, J
   60 T(m) = T(m) + exp(A(j,m))
   70 CONTINUE
   80 CONTINUE
```

N - - - # of spectral segments

K - - - # of gases

L - - - # of raypaths

I - - - # of spectral calculation boundaries

J - - - # of spectral points in a segment

C - - - Cross section array

A - - = Absorption coefficient matrix

U - - - Masspath matrix

T - - - Integrated transmission array

Figure 5.- Calculation Procedure

LINE-BY-LINE RADIATIVE TRANSFER GEOMETRY

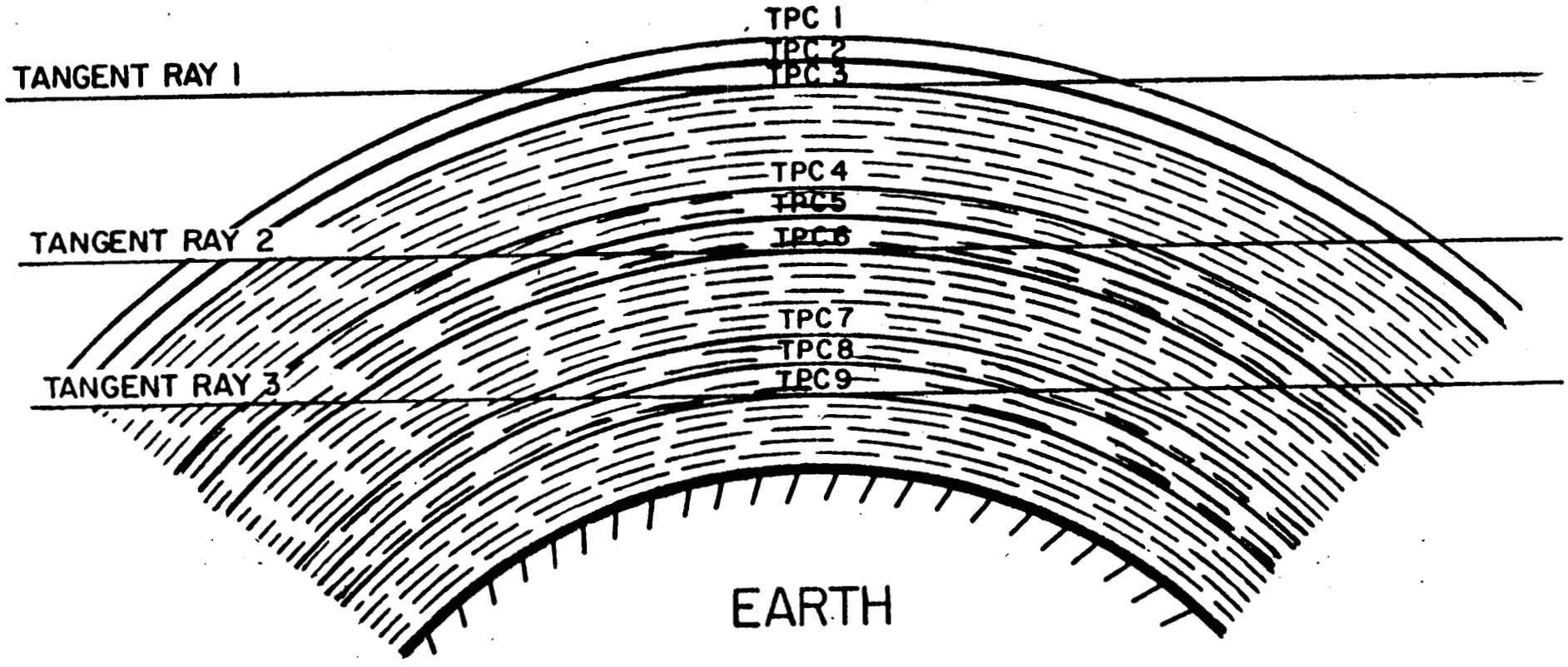

Figure 6

VII. Instrument Characterization Studies

No instrument is theoretically perfect. Therefore imperfections must be characterized through testing and modeling. In the past year William and Mary personnel have performed studies of optical and electronic "cross-talk", detector non-uniformity, and balance off-set effects. These studies are described in the following sections.

VII-1 "Cross-Talk" Effects

"Cross-talk" is an expression used to imply the inseparable mixing of signals. In the HALOE instrument there are two general mechanisms for creating cross-talk; optical reflections and inexact electronic demodulation.

The first, optical cross-talk is caused by radiation being reflected into unintended paths. This causes radiation, nominally intended to fall on a gas (vacuum) path detector, to be particually reflected from at least two elements in such a way that some significant portion of the reflected energy is directed onto a vacuum (gas) path detector.

The second mechanism, electronic cross-talk, causes detector output due to external source radiance (internal black body radiance) to be interpreted as output due to internal black body radiance (external source radiance). The internal black body is used as a constant radiance source for monitoring the relative system attenuation between gas and vacuum paths. When the relative attenuation varies, as detected by a change in the gas-vac reference signal, a gain is applied to the gas path signal by a feed-back loop called the automatic gain control (AGC). The signal due to the internal source is distinguished from external signal sources by chopping the two beams of radiance at 300 hz and 150 hz respectively, then electronically demodulating the signals. Due to unavoidable imperfections in both the chopper and demodulator, there occurs a slight mixing of signals.

VII-1.1 Optical Cross-Talk

Optical cross-talk occurs in a given gas filter correlation channel when a fraction of the signal from one path (gas filter path or vacuum path) is reflected into and interpreted as signal in the other path (vacuum path or gas filter path). The amount of error introduced into the modulation signal by optical cross-talk depends upon two factors: the magnitude and the spectral content of the cross-talked signal.

The HALOE modulation signal, M, is given by:

$M = (GV_g - V_v)/V_{vo}$, where

G = multiplier gain = V_{vo}/V_{go};

V_{vo} = exoatmospheric signal, vacuum path

V_{go} = exoatmospheric signal, gas filter path

V_v = endoatmospheric signal, vacuum path

V_g = endoatmospheric signal, gas filter path

Two types of optical cross-talk were studied. "Gas into vac" (GV) cross-talk occurs when signal from a gas filter path is recorded as signal in the vacuum path. "Vac into gas" (VG) cross-talk occurs when signal from a vacuum path is recorded as signal in the gas filter path.

If only GV cross-talk is present, (values with a prime denote values with cross-talk).

$V_g' = V_g$

$V_{go}' = V_{go}$

$V_v' = V_v + fV_g$

$V_{vo}' = V_{vo} + f_o V_{go}$, and

$M' = (G'V_g' - V_v')/V_{vo}'$

f_o = fraction of energy on gas path detector crosstalked at balance

f = fraction of energy on gas path detector crosstalked during event

Note that f varies with tangent altitude observed.

Expressing M' in terms of the V signals without cross-talk, the following realtion can be otained:

$$M' = \underbrace{\frac{GV_g - V_v}{V_{vo} + f_o V_{go}}}_{1} - \underbrace{\frac{(f - f_o)V_g}{V_{vo} + f_o V_{go}}}_{2} \qquad (1)$$

Term 1 is very nearly the modulation, M, with no cross-talk present. Term 2 represents the source of the greatest modulation error. The fraction of gas path energy crosstalked during the event, f, is greater (assuming a non-negative modulation) than the fraction of cross-talk during balance, f_o. This is because spectral features in the atmosphere correlate with specral features in the GV cross-talk path.

The importance of spectral content in GV cross-talk can be seen in the following Table 4 profiles simulated for the HCl channel of HALOE. The modulation values are expressed in units of noise equivalent modulation, or nem, with 1.0 nem being the desired level of agreement.

TABLE 4

GV x Talk Effects

Tan Height	M_1	M_2	M_3
62	.5198	.520	.5199
50	2.277	2.278	2.271
40	8.657	8.658	8.534
30	27.019	27.022	26.065
20	48.026	48.045	42.181
10	6.298	6.362	-3.623
Crosswalk level:	0.0%	.733%	.505%

Case M_1 has no optical cross-talk and represents the nominal modulation for a standard atmosphere. Case M_2 has optical cross-talk of .733% at balance, and case M_3 has .505% optical cross-talk at balance. However, the cross-talk path for case M_2 was chosen to have a high magnitude but low spectral content. On the other hand, case M_3 has a low magnitude but a high spectal content achieved by a cross-talk path that makes 3 passes through the methane blocking cell. Clearly, modulations M_3 are much differenct from the nominal values M_1 than are the values M_2. These cases illustrated the need to know the origin of the cross-talk in the HALOE instrument if the modulation is to be corrected properly for cross-talk.

VG cross-talk can be analyzed in a manner similar to that for gas into vac cross talk. For vac into gas, define (again, the prime denotes values with cross-talk)

$$V_{vo}' = V_{vo}$$

$$V_{go}' = V_{go} + f_o V_{vo}$$

$$V_v' = V_v$$

$$V_g' = V_g + fV_v$$

$$G' = \frac{V_{vo}'}{V_{go}'} = \frac{V_{vo}}{V_{go} + f_o V_{vo}}$$

$$M' = \frac{G'V_g' - V_v}{V_{vo}'}, \text{ which can reduce to}$$

$$M' = \frac{V_g + fV_v}{V_{go} + f_o V_{vo}} - \frac{V_v}{V_{vo}}$$

If M denotes modulation without cross-talk, the expression for M' can be written

$$M' = \underset{1}{M/(1 + f_o G)} + \underset{2}{\bar{\tau}_V G(f - f_o)/(1 + f_o G)} \qquad (2)$$

where

$$\bar{\tau} \equiv V_V/V_{VO}$$

Here, f_o is the fraction of energy on the vacuum path detector crosstalked at balance; f is the fraction of energy on the vacuum path detector crosstalked during the event. Note that f does not equal f_o except at balance.

Term 1 above is nearly the modulation without cross-talk, as G is on the order of .75, for HCl f_o is on the order of .002.

Term 2 indicates the modulation error introduced by the VG cross-talk, and predicts that all modulation values with only VG will be larger than the modulation values without cross-talk. The Table 5 below lists the results for a VG cross-talk case in the HCl channel for .2% cross-talk at balance.

TABLE 5

VG Cross-Talk Effects

Tangent Heights	M_1(nem)	M_2(nem)
62	0.5198	0.5198
50	2.277	2.278
40	8.657	8.706
30	27.019	27.423
20	48.026	50.351
10	6.298	9.728

Column M_1 represents the nominal modulations for no cross-talk and column M_2 represents the modulations for .2% vac into gas cross-talk. Note all M_2 entries are greater than or equal to M_1 entries as predicted by equation 2. Note the errors are less than 2 nem above 20 km.

It should be pointed out that all atmospheric transmission profiles were calculated using spectral line parameters from the 1982 Air Force Geophysics laboratory tape and line-by-line transmittance code. The HALOE instrument response (i.e., optics transmission) was determined by using vendor supplied transmission curves for all otpical elements.

These simulations of the HCl channel demonstrated the need to reduce the magnitude of any GV cross-talk with high spectral content. The HCl channel is unique in that it contained a methane gas filter in the optical path immediately following the broadband filter. Simulations showed that cross-talked paths making several passes through this cell could be responsible for introducing large modulation errors due to the high spectral content of these paths. To reduce the magnitude of cross-talk paths through the blocking cell, interchanging the location of the blocking cell and broadband filter was proposed. Studies of this new configuration showed that modulation errors due to cross-talk paths through the blocking cell were greatly reduced, due to the reduction in cross-talk magnitude achieved by forcing the cross-talk beam to more than 2 additional passes through the broadband filter. The configuration change was adopted.

During the course of the cross-talk analyses, it was realized that any cross-talk beam will have an effect in both gas and vacuum paths, regardless of its origin. This is because any optical train is divided by a beamsplitter into the gas and vacuum paths, and there is no direct way for any signal reflecting back out of the gas (vac) path to get into the vac (gas) path wihout first encountering the gas-vac beamsplitter. Therefore, any and all cross-talk beams are divided into the vacuum

and gas paths. This should greatly reduce the error in modulations obtained by including cross-talk effects in just on path. In this study we assumed the beam splitter would divide cross-talked energy in the same proportion as primary beam. In reality the reflected energy will favor the direction from which it came due to the polarising effects of the beam splitter. This will further reduced the true cross-talk effects relative to our estimates.

A simulation of gas-vac cross-talk including the component of the beam that remains in the gas path was carried out for a high spectral content and high magnitude (4.5%) cross-talk path in the HCl channel. Listed below in Table 6 are the modulation values calculated.

TABLE 6

Combined Cross-Talk Effect

Tangent Height (km)	M_1 (nem)	M_2 (nem)	M_3 (nem)
62	0.5198	0.5215	0.5202
50	2.277	2.251	2.280
40	8.657	7.630	8.652
30	27.019	18.199	26.895
20	48.026	-2.869	47.063
10	6.298	-68.815	4.100

Once again, M_1 corresponds to the nominal (no cross-talk) modulation level. Case M_2 is the modulation calculated if only the componet of cross-talk split into the vacuum path is included. Note the extremely large changes. Case M_3 is the modulation calculated if both components of cross-talk are included. Note that the agreement is better than any previous case where only one component of cross-talk was studied, especially considering the large magnitude of cross-talk in this last case.

The entire cross-talk anaylsis was significant indefining the importance of the mechanisms (magnitude and spectral content) that contribute to modulation errors of

optical cross-talk is present. The study also resulted in the realization that any cross-talk beam will add to the gas and vacuum path signals, regardless of its origin. Including the cross-talk effects in both gas and vac channels significantly reduced the expected error in modulation and also provided a more accurate representation of the instuments's expected performance.

VII-1.2 Electronic Cross-Talk

The two types of electronic cross-talk are referred to as solar-to-reference and reference-to-solar. In general, the solar-to-reference interferes with the AGC, giving gain correction error and, therefore, $\Delta V/V$ (modulation) error. The reference-to-solar causes a constant offset error in the vacuum and gas path signals, also resulting in modulation error. For a derivation of the electronic cross-talk equations see Appendices B and C.

VII-1.2.1 Solar-to Reference Cross-Talk

The error in modulation $\delta_s M$ due to solar-to-reference cross-talk can be sufficiently approximated by the folowing:

$$\delta_s M = \chi'_v \tau^g [e(1 - \tau^g) - M^m + M_0^m] \qquad (V\text{-}1)$$

where χ'_v is the vacuum path cross-talk level defined as:

$$\chi'_v \equiv (V^m_{rvo} - V_{rvo})/V_{rvo} \qquad (V\text{-}2)$$

Note that reference signal voltage is designated by V_r, instead of R.

V^m_{rvo} is the measured vacuum path reference voltage at balance and V_{rvo} is the measured vacuum path reference voltage while viewing cold space. M^m is the measured modulation, $\Delta V^m/V^m_{svo}$. V^m_{svo} is the measured solar vacuum signal at balance and ΔV^m is the measured ΔV signal (in the same units as V^m_{svo}). M^m_o is measured modulation at balance. $\tau^g \equiv V^m_{sg}/V^m_{svo}$ and can be sufficiently approximated by $(\Delta V^m + V^m_{sv})/V^m_{svo}$. "e" is a system constant that can be determined by the following equation:

$$x'_v e = \frac{(\hat{G} - 1)(1 + \Delta R_o / V_{rvo})}{\hat{G}(M_o + 1)} - x'_v M_o \qquad \text{(V-3)}$$

where $\hat{G}$ is the observed gain, from AGC readout, between balance and space dwell (i.e., $\hat{G} = G_s/G_o$ where G_s = gain at space dwell and G_o = gain at balance). V_{rvo} is the measured vacuum reference signal during space dwell. ΔR_o is the balance ΔR value. Again, voltages must be in the same units; i.e., if ΔR has a gain of 60 over V_{rv}, then ΔR must be divided by 60. Equations V-1 and V-3 can be used in combination with balance and space dwell data to completely define a modulation correction during track mode due to solar-to-reference cross-talk.

Preliminary estimates of the effect of solar-to-reference cross-talk can be found in Table 7.

VII.-1-2-2 Reference-to-Solar Cross-Talks

The error in modulation, $\delta_R M$ due to reference-to-solar cross-talk, is suffi- approximated by:

$$\delta_R M = y_v'[(1 - \tau^g)d - M^m] \qquad \text{(V-4)}$$

y_v' is the vacuum path cross-talk level defined by:

$$y_v' = \frac{V^m_{svo} - V_{svo}}{V_{svo}} = V^m_{sv}(off)/[V^m_{svo} - V^m_{sv}(off)] \qquad \text{(V-5)}$$

where $V^m_{sv}(off)$ is the vacuum path solar measurement while dwelling on cold space (off the Sun). τ^g and M^m are defined as before. "d" can be found by

TABLE 7 - ESTIMATED EFFECT OF SOLAR TO REFERENCE CROSS-TALK

ALT., km		CH_4	HCℓ	NO	HF
62	$\bar{\tau}_g$	.99999	.99996	.99863	.99994
	M	.269	.517	.045	.11
	A	-.0022	-.018	--	-.002
	B	-.0002	-9.2×10^{-4}	--	--
50	$\bar{\tau}_g$	.99960	.9985	.9952	.9995
	M	14.53	2.26	16.17	.72
	A	-.13	-.038	--	-.015
	B	-.01	-.034	--	--
40	$\bar{\tau}_g$	.9946	.9892	.9896	.9986
	M	201.68	8.74	84.61	3.39
	A	-2.0	-.132	--	.077
	B	-.12	-.247	--	--
30	$\bar{\tau}_g$	.9739	.9607	.9707	.9964
	M	815.02	28.45	164.27	11.95
	A	-7.84	-.472	--	-.270
	B	-.52	-.884	--	-.093
20	$\bar{\tau}_g$	.8952	.8499	.8930	.9887
	M	2921.96	43.40	94.96	23.45
	A	-25.84	-.637	--	-.528
	B	-1.93	-2.938	--	-.310
10	$\bar{\tau}_g$	.5838	.4728	.4821	.9007
	M	6775.10	-45.65	42.17	35.23
	A	-39.1	.372	--	-.722
	B	-5.0	-5.745	--	-2.356
6	$\bar{\tau}_g$	--	--	.0176	.472
	M	--	--	--	--
	A	--	--	--	--
	B	--	--	--	--

$\bar{\tau}_g$ = Average gas channel atm. transmission; M = Modulation (NEM)

$A = -\chi\bar{\tau}_g M(NEM)$; $B = \chi_e\bar{\tau}_g(1 - \bar{\tau}_g)$

$$d = \frac{M^m(off)}{y_v'} \qquad (V\text{-}6)$$

where $M^m(off)$ is the measured modulation while dwelling on cold space. Equations V-5 and V-6 can be used in combination with balance and off-Sun data to define a correction to the track mode data, necessitated by reference-to-solar cross-talk. For a detailed derivation of the electronic cross-talk equations, see appendices B and C.

VII-2. Balance Offset Effects

As was seen in section III, the HALOE instrument balances the gas and vaccum path solar signals so that the voltage difference in outputs is zero. This balance operation is performed while viewing unattenuated solar energy, that is, viewing the sun exostmospherically. The signals are matched by applying a gain to the gas path signal. After the balance, the solar signals will change due to atmospheric absorption during sunset or sunrise. Therefore, in order to maintain this balanced condition, an unattenuated internal blackbody reference signal is monitored and maintained at its balance level by varying the gain on the gas path signal. This reference signal is produced by passing the blackbody emission radiance through the same optics as the solar input, to the extent possible. It is chopped at a different frequency than the solar input in order to separate solar from reference through demodulation electronics.

The succesful maintenance of balance depends on several factors. First, the changes in instrument response to gas and vacuum signals must be the same for both reference and solar sources. The variation of system response must not be to fast for the AGC to follow. Finally, the required gain changes must not go past system capabilities.

This last requirement is important when considering initial gain settings and balance resolution. Ignoring cross-talk, the reference and solar difference signals can be modeled with the equations

$$\Delta R = GR_g - R_v$$

$$\Delta V = GV_g - V_v$$

where R_g - reference gas path signal

R_v - reference vac path signal

V_g - solar gas path signal

V_v - solar vac path signal

G - adjustable gain.

The instrument is initially set, in the lab, so that $\Delta R = \Delta V = 0$ for $G = 1$. G is allowed to vary, as needed during the mission, from .75 to 1.25. However, ΔR is digitizied and monitored only over a range $\pm$ .03 R_{VL} where R_{VL} is the initial laboratory setting of R_v.

The balance is maintained over an event by adjusting G so that

$$G = (\Delta R_o + R_v)/R_g$$

where ΔR_o is the balance value of ΔR. If $\Delta R_o = 0$ it is easy to see that ΔV_o would be maintained at zero for any instrumental signal path response change in the form:

$$V_g \rightarrow K_g V_G$$

$$R_g \rightarrow K_g R_g$$

and/or

$$V_v \rightarrow K_v V_v$$

$$R_v \rightarrow K_v R_v$$

This is not the case however, if the K_g and/or K_v are different for reference and solar signals. One must also consider the balance procedure. At balance, G is adjusted to set $\Delta V_o = 0$, i.e.

$$G = (\Delta V_o + V_v)/V_g$$

Where ΔV_o and V_g are the prebalance exatmospheric values.

If K_g and K_v vary by 3% or more between reference and solar signals, ΔR may move outside of its digitization limits. The system balancing technique requires that ΔR remain within the digitization limits. One can change these limits and/or balance away from 0 (i.e. $\Delta V_o \neq 0$) but this will cause necessay corrections to the data.

One more consideration that should be addressed is what is the impact of an imperfect AGC? In other words, can corrections be made for the effects of ΔR not being maintained at the balance condition.

Appendix D addressed these questions resulting in the following correction formula:

$$\delta_B M = \frac{\delta R(M^m + \tau^v) + (R_v^m - R_{vo})\ (M^m - \tau^v\ \Delta R^m/R^m_v)}{\Delta R^m + R^m_v} \qquad \text{(V-7)}$$

$\delta_B M$ - Correction to the measured modulation to obtain the true modulation

M^m - measured modulation $\Delta V/V_{vo}$

τ^V - V_v^m/V_{vo}

V_{vo} - vacuum solar signal at balance

V_v^m - vacuum solar signal

R_{vo} - vacuum reference signal at balance

R_v^m - vacuum reference signal

ΔR^m - delta R signal

δR - $(\Delta R^m - \Delta R_o)$ where $\Delta R_o = \Delta R^m$ at balance

Note that equation V-7 contains only measured quantities.

Primary points of interest are:

1. Failure to maintain the balance condition ($\delta R \neq 0$) can be corrected to the 1 NEM level since $\delta R/(R_v^m + \Delta R^m)$ should be known to 1 NEM as long as ΔR stays within the digitization range.

2. The effects of large off-sets in ΔR at balance are small if $\left|(R_v^m - R_{vo})/(\Delta R^m + R_v^m)\right| \simeq \left|K_v - 1\right|$ is small. For example, if ΔR^m varied by its full range of 0.03, then a 1 NEM or greater effect would require

$$\left|K_v - 1\right| > (2 \times 10^{-5}/.03) \simeq 33 \text{ NEM}$$

The determination of $K_v - 1$ should be accurate to $5 \times 10^{-4}(1/2000)$ which is 25 NEM. Therefore, consideration should be made to extend the range of ΔR.

3. Equation V-7 assumes negligible change in the ratio

$$\left(\frac{K_g(\text{ref})}{K_g(\text{solar})} \cdot \frac{K_v(\text{solar})}{K_v(\text{ref})}\right)$$

during an event.

4. If $\delta R = 0$ (AGC maintains $\Delta R^m = \Delta R_o$) then $\delta_B M = 0$ if $K_v = 1$. It is insensitive to K_g.

VII-3. Correction Formula Interdependence

The modulation error formulas derived in appendices B, C, and D apply for SRXT (Solar to Reference Cross-talk), RSXT (Reference to Solar Cross-talk) and balance related errors, respectively. These derivations were done independently; but, in reality, are interrelated. The effect of SRXT on the RSXT error formula is negligible, as can be seen by formulas C20 and C21. However, all three formulas have terms that are dependent on the measured modulation, implying that the corrections must be a small fraction of the modulation to be valid when used independently. Reviewing the correction formulas, we have:

SRXT Correction:

$$\delta_S M = \chi'_V \tau^g [e(1 - \tau^g) - M^m + M_o^m] \qquad (A)$$

RSXT Correction:

$$\delta_R M = y'_V [(1 - \tau^g)d - M^m] \qquad (B)$$

Balance Related Correction:

$$\delta_B M = \frac{\delta R(M^m + \tau^V) + (R_V^m - R_{VO})(M^m - \tau^V \Delta R^m / R_V^m)}{(\Delta R^m + R_V^m)} \qquad (C)$$

An important point to remember is that the SRXT and BR (Balance Related) formulas are caused by AGC driven gain changes (except for the δR term). One is induced by variation in the SRXT signal, the other is induced by system response changes in the gas and vacuum paths. However, SRXT changes and system response changes can both cause variation in the apparent vacuum reference signal, i.e.,

$$(R_V^m - R_{VO}) \neq 0$$

This suggests the question, will correction C include any part of correction A? The answer is, yes. Since R will change due to the varying SRXT signal during an event, $R_V^m - R_{VO}$ will become non-zero without K_g or K_V deviating from 1. This should be accounted for in the following way.

The portion of $R_v^m - R_{vo}$ due to cross-talk is:

$$\chi'_v R_{vo}(\tau^v - 1)$$

To remove the effect of cross-talk from equation C, one should replace it with equation D10A from appendix D

$$\delta_B M = \frac{\delta R[M^m + \tau^v]}{(\Delta R^m + R_v^m)} + \frac{[R_v^m - R_{vo} - \chi'_v R_{vo}(\tau^v - 1)] \cdot (M^m - \tau^v \Delta R/R_v^m)}{(\Delta R^m + R_v^m)} \qquad (C')$$

The validation of these equations must ultimately come from static model calculations, lab data analysis, and orbital performance. The first two are in progress.

One final comment on these correction formulas--it would be aesthetically satisfying if a formula that rigorously couples the three effects could be derived. The difficulty with attempts at a general formulation is the complexity of the algebra. The cross terms make it difficult to identify terms that can be reliably neglected. It is also difficult to put in a form that includes only telemetered parameters. Indications from preliminary validation efforts are that a general formulation will be unnecessary.

It should be noted that the time dependence of the AGC response will tremendously impact the application of the above correction formulas. These formulas are valid for direct use only in a static situation, which will be virtually non-existent during the mission. However, they serve as tools for understanding the HALOE response and basic building blocks for a dynamic correction.

The point should be made that if all gain changes during an event are determined to be false (i.e., due to cross-talk and system balancing imperfections), then the ΔAGC can be used to develop a simple scale factor correction in addition to the direct use of equation B.

Appendices B, C, and D can also be used to develop more exact corrections, should cross-talk and imbalance become large.

A final point worth considering is a planned calibration sequence for HALOE during high β angle (no sunset) times to determine system response changes as a function of time and temperature. The full, unattenuated Sun can be observed for extended continuous time periods to calibrate system response changes. These calibration curves can then be used in combination with cross-talk corrections during occultation events. Cross-talk changes as a function of time could be determined by periodically scanning off the Sun during these calibration opportunities as well.

In conclusion, we feel that undesired system response characteristics as a function of time and temperature can be determined and monitored in orbit. However, it is critical that these responses be well understood, characterized and minimized through a thorough instrument test campaign in the lab.

VIII. Detector to Beam Non-uniformity Studies

Other processes which may induce modulation errors are beam movement on the detectors as well as the spatial uniformity of the input beam and detectors.

Beam movements may induce modulation errors in the following way. If a detector has a non-uniform response versus position over its active area, moving the beam to another location on the detector may make the signal out of that detector increase or decrease, depending on how the average response of the illuminated detector area changes. Thus, the same input radiance may give many different outputs if the beam moves on a detector having non-uniform spatial response. Beam movements could be very critical to HALOE, since the response from two detectors is differenced to determine the signal (modulation), and slight (1 percent) changes in responsivity can induce a signal error 500 times greater than the noise.

Detector uniformity data are available in the form of response versus position across the active area of each HALOE detector. The data is spaced every 24 micrometers and was produced by a laser spot scan across the detector. The response of a detector for a nominal sized input beam (of diameter 360 μm) is just the average of the spot scan responses in the area filled by the input beam.

Studies were done moving the beam a maximum of 24 microns to the left, right, above, and below detector center for all four gas filter channels, gas and vacuum paths. To study movements of less than 24 microns, the spot scan data were linearly interpolated. For simplicity, both gas and vacuum beams were assumed to move in the same directions, and by the same amount. A standard radiance and modulation profile was used as the nominal response for beams centered on their detectors. To simulate the effects of beam movement, the gas and vacuum path radiances were adjusted by the percentage response change from the center position to the new location. Modulations were then calculated using the new radiances with the multiplier gain calculated for

the nominal conditions. Using the nominal multiplier gain assumes the beam movements are too fast for the Automatic Gain Control to account for.

Below, in table 7, is a list of expected modulation values for each HALOE gas filter correlation channel at 20-km tangent height, for a movement of 1 micron. The center value is the nominal modulation level in NEM. These studies show that small (1 micron or less) movements can induce modulation errors on the order of several NEM, depending on the direction of beam motion. The methane (CH_4) channel appears to be affected least by the movements. This is because the two detectors for this channel are more uniform than the other detectors, and both gas and vacuum path detector responses change about the same amount for a given movement.

This study was undertaken in part as an effort to identify possible sources of noise observed in the instrument.

Table 7

V Signal Change for 1-μm Beam Movement

The following is a list of modulations calculated for a 1-μm beam movement:

	91.752 ↑		
117.358 ←	87.719 →	57.398	NO channel
	↓ 81.224		
	38.386 ↑		
36.327 ←	48.026 →	48.498	HCℓ channel
	↓ 46.315		
	2988.595 ↑		
2987.530 ←	2987.705 →	2987.020	CH_4 channel
	↓ 2987.425		
	34.025 ↑		
34.346 ←	22.981 →	23.651	HF channel
	↓ 48.169		

The second study concerning accurate determination of the HALOE modulation signals was prompted by laboratory measurements of noise and deals with the possibility of beam non-uniformities being imaged on the detector. This will occur if the instrument is not properly focused. In particular, if beam non-uniformities exist, and if those uniformities vary with time, then signal variations may be produced. The cause of beam fluctuations would most likely be a fluctuating amount of water vapor in the 10-m path between the laboratory radiation source and the instrument. The NO channel is most susceptible to water vapor absorption, as a 10-m unpurged path absorbs about 14 percent. Absorption in the 10-m unpurged path for the other three gas filter correlation channels is about 1 percent or less. Non-uniformities arise if the amount of water varies within the beam and across its diameter. It should be pointed out that the absolute absorption level is not important in producing signal variations but it is the range of absorption over the beam diameter that produces signal variations. In addition, the NO channel detectors have the largest spatial non-uniformities of the four gas filter correlation channel detector pairs. Varying beam uniformity on a non-uniform detector will also yield modulation fluctuations, even if the average beam intensity remains constant.

To simulate beam intensity, non-uniformities and the resulting modulation signals, the detector spot scan data was used again. It was assumed that the beam is on the center of the detector and that it doesn't move. Instead of taking a uniformly weighted average of the detector response over the area filled by the beam, a weighted average of the detector response was calculated, with the weights being between τ_L and 1.0, where τ_L represents the lowest transmittance in the 10-m path for a given laboratory relative humidity. The procedure was as follows:

For each of the four gas filter correlation channels:

1. Determine τ_L for various relative humidities.

2. Generate, using a random number generator, a set of weights (beam non-uniformities) between τ_L and 1.0.
3. Calculate the weighted average of the gas filter and vacuum path detectors. This represents the 'balance' conditions. From these conditions, the ratio of the gas and vacuum path responses (V_{vac}/V_{gas}) represents the multiplier gain, G.
4. Generate another set of weights between τ_L and 1.0.
5. Calculate another set of responses for both the gas filter and vacuum path detectors.
6. Multiply the gas filter detector response from step 5 (above) by G and subtract the vacuum path response from step 5 (above). This represents the quantity $GV_g - V_v$ in the numerator of the modulation equation.
7. Multiply $GV_g - V_v$ by 60. (This simulates the magnitude of ΔV as the HALOE instrument would output).
8. Convert the ΔV to counts, between 0 and 4095 for ΔV between ± 5 volts.
9. Repeat steps 4 through 8 three hundred times to simulate 5 minutes (300 seconds) of HALOE telemetry data.
10. Plot the ΔV for each simulated 5-minute run.

Simulations for the NO channel were carried out for τ_L values of 0.85, 0.9, 0.95, 0.98, 0.99, and 0.995. The case for $\tau_L = 0.99$ (i.e., an intensity variation of 1 percent) closely simulated the amount of noise currently observed in the NO channel when the 10-m path is purged with dry nitrogen. The purge path is designed to have a maximum 1-percent relative himidity. Note that for the NO channel, a 10-m path with one percent relative humidity has one percent absorption. As τ_L decreased, the values of ΔV increased.

The CH_4, HCℓ, and HF channels were all simulated at $\tau_L = 0.995$, since the absorption due to water vapor in a 10-m purged path is never greater than about

one-half percent. The simulated δV signals for these three channels produced errors within the currently measured noise levels.

The results of non-uniformity simulations indicate that the NO noise level could be produced by a beam with approximately one percent nonuniformities, assuming the non-uniformities to be 100 percent imaged on the detector face. However, since the aperture stop is intended to be imaged on the detector face, these non-uniformity effects are probably upper limits. On the other hand, a less random non-uniformity model would produce a larger effect. In addition, the absorption variations over the beam are probably overestimated.

Finally, since lab data taken under various conditions of humidity show little change in NO noise levels, beam non-uniformity variation is probably not the source of the noise observed in the NO channel.

IX. Consultation Services

The principal and associate investigators have also served as consultants in many other areas of the HALOE project. Both algorithm development and test review and analysis were involved. A brief description of these tasks follows:

IX-1. HALOE Instrument Testing Support

The past year has seen a comprehensive battery of characterization tests performed on the HALOE instrument. Interpretation of the eventual data set will be critically dependent on the instrument characterization determined by these tests. Therefore, it was necessary for the investigators under this grant to be closely associated with the evaluation of test specifications, procedures, and results.

Specifications were evaluated or derived by estimating the signal sensitivity to the particular instrument function being characterized and requiring that the knowledge of that function allow signal modeling to be accurate to 2 parts in 10^5 (1 NEM).

These evaluations were done using the HALOE spectral instrument model and/or error studies like those presented in appendices B and C.

Test readiness meetings were attended as consultants for help in determining if the test procedures would meet characterization requirements.

Finally, test results were analyzed to determine if objectives were met, both in instrument characterization and performance. Of considerable utility in this process was a plotting code developed by the associate investigator on this grant, for the display and statistical analysis of the HALOE telemetry stream.

Some of the tests involving William and Mary personnel participation were:

1. Filed-of-View Characterization
2. Empty Cell Bias
3. ΔV Bias
4. Balance Linearity

5. Cross-Talk (electrical and optical)
6. Field-of-View Matching
7. Dynamic Range Setting
8. Calibration Wheel Characterization
9. Command Mode
10. Throughput Measurements
11. Gas Response Test

IX-2 Algorithm Development Consultation

The successful processing of the HALOE modulation channel data will require careful attention to the preinverson processing of the telemetered data. The removal of instrument effects, pressure registration, and solar limb darkening curve measurement must be done precisely and accurately. The same is required of the radiometer H_2O channel retrieval since H_2O profiles are necessary for interferrent correction in the modulation channels. The techniques and/or code being implemented to perform these functions originate from work performed by the principal investigator of this grant, although predating this grant. Therefore, the principal investigator's assistance to individuals implementing these functions for HALOE has and will continue to be a significant portion of the contract support.

X. Conclusions

The past year has seen significant progress toward the ultimate goal of successfully inverting the future HALOE data set to desired mixing ratio profiles.

The primary accomplishment has been the detailed definition of the modulation retrieval approach. Besides the definition, critical software modules required by the approach are nearing completion, namely, the Line-by-line code and associated modules for fast Voight function evaluation, interpolation, path integration, and line parameter logistics.

In addition, the application of the EGA technique to production signal simulation has been outlined in detail. The software needed for implementing EGA is in hand. The implementation procedure has been broken into steps equivalent to broad band uses allowing completion of the task in about 2 months. A prototype modulation retrieval package should be operational by early spring of 1987.

A second area of accomplishment was the mathematical characterization of the major signal response errors. Balance offset, ΔR drift, optical cross-talk, solar-to-reference cross-talk, and reference-to-solar cross-talk have all been quantified with in-flight correction procedures defined. It should be noted, validation by the instrument static model and lab data analysis are still needed and will be performed in the coming year.

The final major area of support was in consultation on instrument testing. This involved many hours of meetings as well as test result analyses.

The coming year should see the successful software completion, testing, and documentation of the modulation channel retrieval algorithm.

Consultation support in the areas of instrument testing and HALOE system software will continue as before.

Appendix A

Modulation Formulations

$$\Delta V = \int Sf\tau_a\tau_c(G\tau_g\tau_1 - \tau_2)d\nu \tag{A1}$$

$$f' = f\tau_c\tau_2$$

$$G' = G\tau_1/\tau_2$$

Equation A1 becomes

$$\Delta V = \int Sf'\tau_a(G'\tau_g - 1)d\nu \tag{A2}$$

Balance equation is

$$\Delta V_B = \int Sf'(G'\tau_g - 1)d\nu \tag{A3}$$

$$\xi_a = 1 - \tau_a$$

$$\xi_g = 1 - \tau_g$$

Equation A2 becomes

$$\Delta V = \int Sf'(1 - \xi_a)[G'(1 - \xi_g) - 1]d\nu$$

or

$$\Delta V = \int Sf'[G'(1 - \xi_g) - 1]d\nu + \int Sf'\xi_a d\nu - \int Sf'\xi_a G'd\nu + \int Sf'\xi_a G'\xi_g d\nu$$

Since

$$\int Sf'[G'(1 - \xi_g) - 1]d\nu = \Delta V_B$$

we have

$$\Delta V = \Delta V_B + \int Sf'\xi_a d\nu - \int Sf'\xi_a G'd\nu + \int Sf'\xi_a\xi_g G'd\nu \tag{A4}$$

for illustrative purposes note that if

$$G' = \text{constant} = \overline{G}$$

which is likely a good approximation, then

$$\int Sf'\xi_a d\nu - \int Sf'\xi_a G' d\nu = (\overline{G} - 1) \int Sf'(1 - \tau_a) d\nu$$

Defining

V_{VO} = Vacuum path measured signal exoatmospherically

V_{VI} = Vacuum path measured signal viewing through atmosphere

Then equation A4 becomes

$$\Delta V \simeq \Delta V_B - (\overline{G} - 1)(V_{VO} - V_{VI}) + \overline{G} \int Sf'\xi_a\xi_g d\nu \qquad (A5)$$

Modulation is normally defined for the HALOE experiment as:

$$M = \Delta V / V_{VO}$$

From the balance equation we see that for $\Delta V_B = 0$ (as with HALOE)

$$\overline{G} = \frac{\int Sf' d\nu}{\int Sf'\tau_g d\nu} \equiv 1/\overline{\tau}_g \qquad (A6)$$

Equation A5 can be seen to be

$$M = \frac{\Delta V}{V_{VO}} \simeq -\left(\frac{1 - \overline{\tau}_g}{\overline{\tau}_g}\right)\left(1 - \overline{\tau}_a^b\right) + \frac{(1 - \overline{\tau}_g)}{\overline{\tau}_g}\left(1 - \overline{\tau}_a^g\right) \qquad (A7)$$

where

$\overline{\tau}_a^b$ = average wide band transmission, or τ_a as weighted by $Sf'/\int Sf' d\nu$

$\overline{\tau}_a^g$ = average gas filter transmission as weighted by $Sf'(1 - \tau_g)/\int Sf'(1 - \tau_g) d\nu$

This points out that the HALOE signal is proportional to the difference between the average absorption over the gas path filter defined by $f'\xi_g$ and the broad filter defined by f'.

Definition of terms in this appendix not previously defined

f = broad band spectral filter

τ_a = atmospheric transmission

τ_c = attenuation common to both gas and vacuum paths

τ_1 = attenuation unique to gas path

τ_2 = attenuation unique to vacuum path

S = source function

G = gain factor applied to gas path to meet balance condition

Appendix B

Solar-to-Reference Cross-Talk

The electronic processing of the HALOE signal from a detector can be modeled as follows (assuming system linearity):

$$V = \omega R F \chi Q \tag{B1}$$

where

V = voltage

ω = watts on detector

R = responsitivity of the detector in amps/watt

F = conversion factor of volts/amp

χ = efficiency at which the a.c. signal is converted (demodulated) to a d.c. signal

Q = a fixed gain, assumed constant

For simplicity we can combine Q and F, assuming they are fixed.

$$C = QF$$

and

$$V = \omega R \chi C \tag{B2}$$

The reference blackbody power on a gas channel detector, interpreted as reference signal, would give a voltage of:

$$V_{rvg} = \omega_{rg} R_{rg} \chi_{rrg} C_{vg} \tag{B3}$$

where subscript r indicates reference, rr indicates reference input to reference signal and g indicates gas channel. Likewise, the reference signal due to solar input in the gas channel would be:

$$V_{srg} = \omega_{sg} R_{sg} \chi_{srg} C_{rg} \tag{B4}$$

Let

$$C'_{rg} \equiv \chi_{rrg} C_{rg} \tag{B5a}$$

$$\chi_g \equiv \chi_{srg}/\chi_{rrg} \tag{B5b}$$

and

$$A_{rg} \equiv \omega_{rg} R_{rg} \tag{B5c}$$

$$A_{sg} \equiv \omega_{sg} R_{sg}$$

Then

$$V^m_{rg} \equiv V_{rrg} + V_{srg} = A_{rg} C'_{rg} + \chi_g A_{sg} C'_{rg}* \tag{B6}$$

In reality HALOE does not make a V^m_{rg} measurement, therefore, this term will eventually be eliminated from our formulas.

The analogous equation for the measured reference signal in the vacuum path would be:

$$V^m_{rv} \equiv V_{rrv} + V_{srv} = A_{rv} C'_{rv} + \chi_v A_{sv} C'_{rv} \tag{B7}$$

where

$$\chi_v = \chi_{srv}/\chi_{rrv}$$

(For the ideal instrument, $\chi_{srg} = \chi_{srv} = 0$)

For this development we will assume no reference-to-solar cross-talk; i.e., $\chi_{rsg} = \chi_{rsv} = 0$. This gives the solar signal equations of

$$V^m_{sg} \equiv V_{ssg} = A_{sg} C'_{sg} \tag{B8a}$$

$$V^m_{sv} \equiv V_{ssv} = A_{sv} C'_{sv} \tag{B8b}$$

We now define f_s and f_r as:

*Superscript m indicates a measured quantity

$$f_s \equiv \frac{C'_{sg}}{C'_{sv}} \tag{B9a}$$

$$f_r \equiv \frac{C'_{rg}}{C'_{rv}} \tag{B9b}$$

also

$$V_{rg} \equiv A_{rg}C'_{rg} = V_{rrg} \tag{B10a}$$

$$V_{rv} \equiv A_{rv}C'_{rv} = V_{rrv} \tag{B10b}$$

It can then be shown that

$$\Delta R^m \equiv V^m_{rg} - V^m_{rv} = V_{rg} - V_{rv} + \chi_v \frac{C'_{rv}}{C'_{sv}} \left[\frac{\chi_g f_r}{\chi_v f_s}(V^m_{sg} - V^m_{sv})\right] \tag{B11}$$

In order to simplify the algebra we will make the following definitions:

$$\hat{\chi}_v \equiv \chi_v C'_{rv}/C'_{sv} \tag{B12a}$$

$$I \equiv (\chi_g f_r)/(\chi_v f_s) \tag{B12b}$$

Designating a balance condition by subscript o equation B11 at balance would be:

$$\Delta R^m_o = V_{rgo} - V_{rvo} + \hat{\chi}_v(IV^m_{sgo} - V^m_{svo}) \tag{B13}$$

At some later time the measured solar signals change while ΔR^m is held constant by applying a gain we will call G to the gas channel signal

$$\Delta R^m = \Delta R^m_o = GV_{rgo} - V_{rvo} + \hat{\chi}_v(IV^m_{sg} - V^m_{sv}) \tag{B14}$$

Note that V_{rgo} is a constant voltage while V^m_{sg} is a changing measurement that includes both G and atmospheric effects; i.e., $V^m_{sg} = GA_{sg}C'_{sg}$. Subtracting equation B14 from B13 and solving for G gives:

$$G = [V_{rgo} + \hat{\chi}_v(V^m_{sv} - V^m_{svo}) + \hat{\chi}_v I(V^m_{sgo} - V^m_{sg})]/V_{rgo} \tag{B15}$$

The error in modulation δM is the difference between measured modulation less modulation for $G = 1$. Remember, G is implicitly contained in V^m_{sg}.

$$\delta M = (V^m_{sg} - V^m_{sv})/V^m_{svo} - (V^m_{sg}/G - V^m_{sv})/V^m_{svo} = (GV^m_{sg} - V^m_{sg})/(GV^m_{svo}) \tag{B16}$$

Substituting B15 into B16 gives

$$\delta M = \frac{V^m_{sg}\hat{\chi}_v}{GV^m_{svo}V_{rgo}} [I(V^m_{sgo} - V^m_{sg}) - (V^m_{svo} - V^m_{sv})] \tag{B17a}$$

Defining

$$e \equiv I - 1 \tag{B17b}$$

and assuming $M^m = M^m_o$ at balance, equation B17 becomes

$$\delta M = \frac{\hat{\chi}_v V^m_{sg}}{GV_{rgo}} [e(V^m_{sgo} - V^m_{sg})/V^m_{svo} - M^m + M^m_o] \tag{B18}$$

To determine the magnitude of this error, $\hat{\chi}_v$, e and G must be measured or calculated.

In the lab, a cross-talk value χ'_v is measured by balancing the instrument while viewing a laboratory black body and recording a measurement for V^m_{rvo}. The input is then shuttered-off causing the V^m_{rvo} which is recorded. χ'_v is then defined as:

$$\chi_v' \equiv (V^m_{rvo} - V_{rvo})/V_{rvo} \tag{B19}$$

from equation B13, this can be seen to be

$$\chi_v' = \hat{\chi}_v V^m_{svo}/V_{rvo} \tag{B20}$$

Substituting B20 into B18 gives

$$\delta M = \left(\frac{V_{rvo}}{GV_{rgo}}\right) \frac{\chi_v' V^m_{sg}}{V^m_{sgo}} [e(V^m_{sgo} - V^m_{sg})/V^m_{sgo} - M^m + M^m_o] \tag{B21}$$

Defining $\tau^g \equiv V^m_{sg}/V^m_{sgo}$ and setting $V_{rvo}/(GV_{rgo}) \simeq 1$, equation B21 becomes

$$\delta M \simeq \chi_v' \tau^g [e(1 - \tau^g) - M^m + M^m_o] \tag{B23}$$

Two tasks remain before B23 can be used. The validity of B22 must be established (this will be done later) and e must be determined for each channel. e can be found directly if one scans off the Sun after balance, dwelling on deep space until the AGC (automatic gain control) drives ΔR back to ΔR_o by applying an additional gain of $\hat{G}$. From equation B13 we would have, off the Sun:

$$\Delta R^m = \hat{G} V_{rgo} - V_{rvo} = \Delta R_o \tag{B24}$$

Multiplying equation B13 by $\hat{G}$, substracting it from B24, and solving for I gives

$$I = \frac{V^m_{svo}}{V^m_{sgo}} + \frac{(\hat{G} - 1)}{\hat{G}} \frac{(V_{rvo} + \Delta R_o)}{V^m_{sgo}\hat{\chi}_v} \tag{B25}$$

Since

$$V^m_{svo}/V^m_{sgo} = 1/(1 + M^m_o) \simeq 1 - M^m_o$$

and from B20

$$\hat{\chi} = \chi'_v V_{rvo}/V^m_{svo}$$

B25 goes to:

$$I - 1 = e = \frac{(\hat{G} - 1)(1 + \Delta R_o/V_{rvo})}{\hat{G}\chi'_v(1 + M_o)} - M_o \qquad (B26)$$

From the AGC telemetry one can determine $\hat{G}$ while equation B19 can be used to determine χ'_v. Note $(\hat{G} - 1)/\hat{G} \simeq \Delta G$ incurred from on to off the Sun.

One should note from equations B12a and B20 that

$$\chi'_v = \chi_v C'_{rv} V^m_{svo}/(C'_{sv} V_{rvo}) \qquad (B27)$$

This shows that the cross-talk value $\chi'_v \simeq V^m_{svo}$ (other parameters stay nearly constant regardless of input). This means that the orbital cross-talk effect will be larger than experienced in the lab. Also note that

$$I \equiv \frac{\chi_g f_r}{\chi_v f_s} = \frac{\chi_g C'_{rg} C'_{sv}}{\chi_v C'_{rv} C'_{sg}} \qquad (B28)$$

or from B8a through B10b

$$I = \frac{\chi_g V_{rrgo} A_{rvo} A_{sgo}}{\chi_v V_{rrvo} A_{rgo} A_{svo}} \qquad (B29)$$

From B29 we see that I is constant, so we will find a relation for a perfectly balanced system (i.e., $M_o = 0$ and $\Delta R^m_o = 0$). One can show from equations B13 and B19 that:

$$\frac{V_{rgo}}{V_{rvo}} = 1 - (\chi'_v e)$$

for $\chi_v' \ll 1$ and $\chi_g = \chi_v$, then

$$I \simeq \frac{A_{rvo}A_{sgo}}{A_{rgo}A_{svo}} \tag{B30}$$

when the system is balanced. The A's are amps out of the detectors at balance due to reference and solar watts on the detectors. These ratios can be obtained directly from Bob Spiers throughput measurements and are included in Table B1. Note that the assumption of $\chi_g = \chi_v$ is not reliable and, therefore, I should be determined by dwelling off the Sun.

TABLE B1.- CROSS-TALK PARAMETER ESTIMATES

Channel	A_{svo}/A_{sgo}	A_{rvo}/A_{rgo}	e	$\chi_v'(2680)$	$\frac{\chi_v'(6000)}{\chi_v'(2680)}$	$\chi_v'(6000)$
NO	.5650	.5714	.011	.0003	3.41	.001
CH_4	1.272	1.2187	-.042	.0024	4.13	.010
HCℓ	.7695	.7485	-.027 (-.040)	.0028	4.17	.012
HF	.7855	.7676	-.023	.9943	5.31	.023

The $\chi_v'(2680)$ values were measured in the lab. The $\chi_v'(6000)$ value is the predicted level of cross-talk that will be encountered in orbit. It is also estimated that e for the HCℓ channel will change from lab estimates due to the difference in the solar and lab Planck curves as weighted over the gas cell. The solar value is enclosed in parentheses. Other channels are predicted to incur little change.

One final task is to show the validity of B22. This is done by first observing that equation B14 is

$$\Delta R^m = GV_{rgo} + \chi_v(IV^m_{sgo} - V^m_{sv}) - V_{rvo} \tag{B31}$$

or from B20

$$\frac{GV_{rgo}}{V_{rvo}} = 1 - \chi'_v \frac{(IV^m_{sgo} - V^m_{svo})}{V^m_{svo}} + \frac{\Delta R^m}{V_{rvo}} \tag{B32}$$

$$\frac{GV_{rgo}}{V_{rvo}} = 1 - \chi'_v M^m + \chi' r\tau^g + \frac{\Delta R^m}{V_{rvo}}$$

Using values in Table 2, Table B1, and a balance within ΔR range of 1/60 of V_{rvo}

$$\frac{GV_{rgo}}{V_{rvo}} - 1 < \chi'(e\tau^g - M^m) + \frac{\Delta R^m}{V_{rvo}} < .016$$

This proves that

$$\frac{GV_{rgo}}{V_{rvo}} \approx 1 \qquad \frac{V_{rvo}}{GV_{rvo}} \approx 1$$

and that the error in δM due to this assumption is less than 1.6 percent of δM.

Since this appendix was written, it has been determined that χ'_v can be quite different for the ΔR demodulation. This negates the use of B19 for the determination of χ'_v. However, $\chi'_v e$ can be determined by the use of B26 since from B26

$$\chi'_v(e + M_o) \approx \chi'_v e \approx \frac{G - 1}{\hat{G}} \frac{(1 + \Delta R_o/V_{rvo})}{(1 + M_o)} \tag{B33}$$

For a balance near zero, the correction equation B23 can be approximated by

$$\delta M \approx \chi'_v e\tau^g(1 - \tau^g) \tag{B34}$$

In addition, if equation B30 is used in conjunction with throughput measurement of e, B33 can be used to infer χ'_V. However, it is hoped that B34 will be an adequate correction, which will be the case if cross-talk does not increase dramatically from lab levels.

For the static case, these corrections have been verified with the static model, but under the assumption that the ΔR and R cross-talk mechanisms are identical. The dynamic case will cause a greater effect. Since the gain change, when input is blocked, is $\hat{G} - 1 \approx \chi'_V e$, the error in gain at sunrise will be $\chi' e$. For low beta angles, the complete event may be only one or two AGC time constants long, preventing the gain from returning to balance conditions. From Table B1, we see that this can be on the order of a 20 NEM error, from lab measurements. However, the χ'_V values are currently larger than listed in Table B1 due to the ΔR versus R demodulation differences as mentioned above. It is hoped that setting the demodulation phase by minimizing ΔAGC change, when input is shuttered, will improve the effective cross-talk. In any case, a time dependent correction will be needed. This may be as simple as a direct use of the ΔAGC, if other gain change causes are negligible.

Appendix C

Reference-to-Solar Cross-Talk

In order to follow this analysis, a thorough review of Appendix B is required.

Equations analogous to B3 through B56 would be:

$$V_{ssg} = W_{sg}R_{sg}X_{ssg}C_{sg} \tag{C1}$$

$$V_{rsg} = W_{rg}R_{rg}X_{rsg}C_{sg}$$

$$C'_{sg} = X_{ssv}C_{sg} \tag{C3}$$

$$Y_g = X_{rsg}/X_{ssg} \tag{C4a}$$

$$Y_v = X_{rsv}/X_{ssv} \tag{C4b}$$

The equations analogous to B6 and B7 would be:

$$V^m_{sg} = V_{ssg} + V_{rsg} = A_{sg}C'_{sg} + Y_gA_{rg}C'_{sg} \tag{C5}$$

$$V^m_{sv} = V_{ssv} + V_{rsv} = A_{sv}C'_{sv} + Y_vA_{rv}C'_{sv} \tag{C6}$$

Equation B11 and B12 equivalents would be:

$$\Delta V^m \equiv V^m_{sg} - V^m_{sv} = V_{sg} - V_{sv} + Y_v\frac{C'_{sv}}{C'_{rv}}\left[\frac{Y_gf_s}{Y_vf_r}V_{rgo} - V_{rvo}\right] \tag{C7}$$

$$\hat{y}_v = y_vC'_{sv}/C'_{sv} \tag{C8}$$

Defining

$$J = (Y_gf_s)/(Y_vf_r)$$

Equation C7 becomes

$$\Delta V^m = V_{sg} - V_{sv} + \hat{y}_v(JV_{rgo} - V_{rvo}) \tag{C9}$$

If J is very nearly 1 and $d \equiv J - 1$, at balance

$$\Delta V_o^m = V_{sgo} - V_{svo} + \hat{y}_v[(1 + d)V_{rgo} - V_{rvo}] \tag{C10}$$

Now define H such that

$$\Delta V_o^m = HV_{sgo} - V_{svo} \tag{C11}$$

Subtracting C11 from C10 and solving for H

$$H = 1 + Z/V_{sgo} \tag{C12}$$

where

$$Z = \hat{y}_v[(1 + d)V_{rgo} - V_{rvo}] \tag{C13}$$

The measured modulation without cross-talk would be

$$M = [(1 + Z/V_{sgo})V_{sg} - V_{sv}]/V_{svo} \tag{C14}$$

Measured modulation with cross-talk:

$$M^m = (V_{sg} - V_{sv} + Z)/V_{svo}^m \tag{C15}$$

The lab measured cross-talk y_v' is:

$$y_v' = (V_{svo}^m - V_{svo})/V_{svo} \tag{C16}$$

C15 can be written as:

$$M^m = (V_{sg} - V_{sv} + Z)/V_{svo} - y_v'M^m \tag{C17}$$

The error in modulation is (C17 - C14):

$$\delta M = M^m - M = Z(1 - V_{sg}/V_{sgo})/V_{svo} - y_v'M^m \tag{C18}$$

Defining $\tau^g = V_{sg}/V_{sgo}$, C18 becomes

$$\delta M = \hat{y}_v(1 - \tau^g)\left(\frac{V_{rgo} - V_{rvo} + dV_{rgo}}{V_{svo}}\right) - y'_v M^m \qquad \text{(C19a)}$$

Since $y'_v = \hat{y}_v V_{rvo}/V_{svo}$, equation C19 becomes

$$\delta M = y'_v\left[(1 - \tau^g)\left(\frac{V_{rgo} - V_{rvo}}{V_{rvo}} + \frac{dV_{rgo}}{V_{rvo}}\right) - M^m\right] \qquad \text{(C20)}$$

From equations B13 and B20, one can show that

$$\frac{V_{rgo} - V_{rvo}}{V_{rvo}} = \chi'_v e \frac{V^m_{svo}}{V^m_{svo}} = \chi'_v e \qquad \text{(C21)}$$

and, therefore

$$\frac{V_{rgo}}{V_{rvo}} = \chi'_v e + 1$$

From Table B1, it is apparent that C20 can be approximated by

$$\delta M \simeq y'_v[(1 - \tau^g)d - M^m] \qquad \text{(C22)}$$

Observe from definitions of J and I that if $\chi_g = \chi_v$; $y_g = y_v$; $J \simeq 1$ and $I \simeq 1$, then $d \simeq -e$.

Table C1 shows y'_v values for each channel, both lab and estimated orbital levels. The d values are simply the negative e values from Table B1.

TABLE C1.- REFERENCE → SOLAR CROSS-TALK

Channel	y'_v 2680 K	y'_v 6000 K	d 6000 K
NO	-.003	-.0088	-.011
CH_4	.002	.0005	.042
$HC\ell$	.002	.0003	.040
HF	.0025	.0005	.023

Note that y'_v for NO is negative. This is not unexpected. Demodulation phase errors can cause negative signals. Also note that y'_v is inversely proportional to input radiance levels.

In order to find d operationally, use the following development. At balance:

$$\Delta V_o = V^m_{sgo} - V^m_{svo} = V_{sgo} - V_{svo} + \hat{y}_v(JV_{rgo} - V_{rvo}) \tag{C23}$$

Off the Sun:

$$\Delta V^m = V^m_{sg} - V^m_{sv} = \hat{y}_v(J\hat{G}V_{rgo} - V_{rvo}) \tag{C24}$$

$$\Delta R^m = V^m_{rg} - V^m_{rv} = \hat{G}V_{rgo} - V_{rvo} = \Delta R_o \tag{C25}$$

where $\hat{G}_m$ is the same gain described in Appendix B, that which must be applied to hold $\Delta R = \Delta R_o$.

From the definition of y'_v

$$y'_v = V^m_{sv}(\text{off Sun})/(V^m_{svo} - V^m_{sv}(\text{off Sun})) \tag{C26}$$

from C25

$$V_{rgo} = (\Delta R_o + V_{rvo})/\hat{G}$$

Substituting C27 into C24:

$$\Delta V^m(\text{off Sun}) = \hat{y}_v[J(\Delta R_o + V_{rvo}) - V_{rvo}] \tag{C28}$$

From C19b and C28, making use of C19b

$$\frac{\Delta V^m}{y'_v V_{svo}} = \frac{J(\Delta R_o + V_{rvo})}{V_{rvo}} - 1 \tag{C30}$$

Now making use of the relationships

$$V_{svo} = V^m_{svo}/(y'_v + 1) \tag{C31a}$$

and

$$V_{rvo} = V^m_{rvo}/(x'_v + 1) \tag{C31b}$$

We have, using the definition of $J \equiv d + 1$

$$d = \frac{\dfrac{M^m(y'_v + 1)}{y'_v} - \dfrac{\Delta R_o(x'_v + 1)}{V^m_{rvo}}}{1 + \dfrac{\Delta R_o(x'_v + 1)}{V^m_{rvo}}} \tag{C32}$$

of if the balance is such that ΔR_o is within the digitization range of $1/60(V^m_{rvo}$, "d" can be approximated to 1.6 percent by:

$$d \simeq \frac{M^m(y'_v + 1)}{y'_v} - \frac{\Delta R_o(x'_v + 1)}{V^m_{vro}} \tag{C33}$$

for expected levels of ΔR_o, x'_v, and y'_v; i.e., $\Delta R_o/V^m_{rvo} < 1 \times 10^{-4}$ and current estimates of cross-talk.

$$d \simeq \frac{M^m(\text{off Sun})}{y'_v} \tag{C34}$$

or

$$y'_v d \simeq M^m(\text{off Sun}) \tag{C35}$$

A simpler way, going directly from C30 and C16 (since $V_{svo} = V^m_{svo}/(y'_v + 1^m)$)

$$M^m(\text{off}) = \frac{\Delta V^m(\text{off})}{V^m_{svo}} = \frac{y'_v}{y'_v + 1}\left[J\left(\frac{\Delta R}{V_{rvo}} + 1\right) - 1\right]$$

Since $d \equiv J-1$, then

$$M^m(\text{off}) \simeq \frac{y'_v}{y'_v + 1}\left(\frac{J\Delta R}{V_{rvo}} + d\right) \simeq y'_v d$$

We should point out that the simplest way of correcting for this reference-to-solar cross-talk error would be to subtract the $M^m(\text{off Sun})$ value from the measured modulation. Any resulting balance offset is treated accordingly. The above development is useful in determining the magnitude of the expected modulation error if cross-talk is neglected.

APPENDIX D

ΔR Offset Effect on Modulation

At balance

$$\Delta R_o = R_{go} - R_{vo} \tag{D1}$$

where

ΔR_o = measured gas-vacuum reference signal at balance

R_{vo} = measured vacuum path reference signal

R_{go} = gas path reference signal

At some time after balance

$$\Delta R_o^m \rightarrow \Delta R^m = GK_gR_{go} - K_vR_{vo} \tag{D2}$$

where

K_g = a system response change factor in the gas path

K_v = a system response change factor in the vacuum path

G = a gain applied to the gas path signal in an attempt to maintain ΔR^m at balance value.

Using D1 and D2 to solve for K_g:

$$K_g = (\Delta R^m + R_v^m)/[G(\Delta R_o + R_{vo})] \tag{D3}$$

where

$$R_v^m = K_vR_{vo} \text{ (a measured quantity)} \tag{D3a}$$

If $K_g = K_v = 1$, then no system response change occurs and the true modulation would be measured as:

$$M^T = (V_g - V_v)/V_{vo}^m \tag{D4}$$

V_g = solar gas path signal

V_v = solar vacuum path signal

$V_{vo}^m = V_{vo}$ = measured vacuum path signal at balance.

Assuming system changes occur, and that they have the identical multiplicative effect on solar and reference signals, then the measured modulation would be (Note that cross-talk is ignored.):

$$M^m = (GK_g V_g - K_v V_v)/V_{vo} \tag{D5}$$

We would like to determine a correction factor $\delta_B M = M^m - M^T$, in terms of measured quantities, in order to correct the measured modulation to true modulation values.

$$\delta_B M = M^m - M^T = M^m - \frac{(V_g - V_v)}{V_{vo}} \tag{D6}$$

Using D5 to solve for V_g and substituting D3 for K_g, we have

$$V_g = (M^m V_{vo} + V_v^m)(\Delta R_o + R_{vo})/(\Delta R^m + R_v^m) \tag{D7}$$

where

$$V_v = V_v^m R_{vo}/R_v^m \tag{D8}$$

Now D6 becomes (using D7 and D8)

$$\delta_B M = M^m - \frac{R_v^m(M^m V_{vo} + V_v^m)(\Delta R_o + R_{vo}) - V_v^m R_{vo}(\Delta R^m + R_v^m)}{R_v^m V_{vo}(\Delta R^m + R_v^m)} \tag{D9}$$

Continuing the algebra with the substitution of $\Delta R_o = \Delta R^m - \delta R$ (which defines δR)

$$\delta_B M = M^m - \frac{R_v^m[M^m V_{vo}(\Delta R^m - \delta R) + M^m V_{vo} R_{vo} + V_v^m(\Delta R^m - \delta R) + V_v^m R_{vo} - V_v^m R_{vo}] - V_v^m R_{vo}\Delta R^m}{R_v^m V_{vo}(\Delta R^m + R_v^m)}$$

$$\delta_B M = \frac{M^m \delta R}{(\Delta R^m + R_v^m)} + \frac{M^m V_{vo} R_v^m (R_v^m - R_{vo}) - V_v^m \Delta R^m (R_v^m - R_{vo})}{R_v^m V_{vo} (\Delta R^m + R_v^m)} + \frac{R_v^m V_v^m \delta R}{R_v^m V_{vo} (\Delta R^m + R_v^m)}$$

Further reduction along with the identify

$$\tau^v = V_v^m / V_{vo}$$

gives

$$\delta_B M = \frac{\delta R}{(\Delta R^m + R_v^m)} (M^m + \tau^v) + \frac{R_v^m - R_{vo}}{\Delta R^m + R_v^m} (M^m - \tau^v \Delta R^m / R_v^m) \qquad \text{(D10)}$$

Since $R_v^m - R_{vo}$ is partially due to solar-to-reference cross-talk it must be accounted for. The portion of R_v^m that is due to cross-talk is

$$x_v' \tau^v R_{vo}$$

The portion of $R_v^m - R_{vo}$ that is due to cross-talk is

$$x_v' R_{vo} (\tau^v - 1)$$

and D10 becomes

$$\delta_B M = \underbrace{\frac{\delta R}{(\Delta R^m + R_v^m)} (M^m + \tau^v)}_{\text{AGC error}} + \underbrace{\frac{R_v^m - R_{vo} - x_v' R_{vo} (\tau^v - 1)}{\Delta R^m + R_v^m} (M^m - \tau^v \Delta R^m / R_v^m)}_{\text{Error due to } \Delta R \text{ balance offset}} \qquad \text{(D10a)}$$

Note that the correction accuracy limitation for balance offset comes from one-half bit of R_v^m and R_{vo}. If R_v^m is digitized 0 to 2000 then for 1 NEM accuracy (We have ignored M^m component and denominator error.)

$$\frac{2 \times 1/2}{2000} \tau^{v} \frac{\Delta R^{m}}{R_{v}^{m}} = 2 \times 10^{-5}$$

If $\tau^{v} = 0.5$, we must have

$$\frac{\Delta R^{m}}{R_{v}^{m}} > 0.08$$

before a 1 NEM error effect is incurred.

It is useful to show what happens if system response changes do not afftect both solar and reference signals identically. To do this, we assume that there occurs a system response that affects only the reference signal; i.e., D2 becomes

$$\Delta R^{m'} = GK_{g}'R_{go} - K_{v}'R_{vo} \tag{D11}$$

D5 would be

$$M^{m'} = (GV_{g} - V_{v})/V_{vo} \tag{D12}$$

In this case $V_{g} = V_{g}^{m}$ and $V_{v} = V_{v}^{m}$

$$\delta M' = M^{m'} - M^{T} = M^{m'} - (V_{g} - V_{v})/V_{vo} \tag{D13}$$

Using the same algebra as before:

$$\delta M' = (G - 1)(M^{m'} + \tau^{v}) \tag{D14}$$

In this case G should be monitored using the AGC data. From D11 and the balance equation, D1, it can be shown that

$$G = \frac{\Delta R^{m'} + K_{v}'R_{vo}}{K_{g}'(\Delta R_{o} + R_{vo})} \tag{D15}$$

Or, if $\Delta R^m = \Delta R_o = 0$

$$G = \frac{K_y'}{K_g'} \tag{D16}$$

G is the ratio of the changes in system response for vacuum and gas reference signal, but only when the solar signal responses are unchanged.

A more general description (although not yet adequately developed) is as follows. Let the various response change factors be:

K_{gs} = solar gas

K_{vs} = solar vacuum

K_{gr} = reference gas

K_{vr} = reference vacuum

Then

$$K_g = K_{gs} \tag{D17a}$$

$$K_v = K_{vs} \tag{D17b}$$

$$K_{gr} = K_g K_g'$$

$$K_{vr} = K_v K_v'$$

or

$$K_g' = K_{gr}/K_{gs} \tag{D18a}$$

$$K_v' = K_{vr}/K_{vs} \tag{D18b}$$

If all four individual response change factors were known, then D14 could be used to calculate a new $M^m = M^{m\prime} - \delta M'$ using G obtained from D15 or D16. A new $R_v^m = R_v^{m\prime}/K_g'$ could be calculated. Then the new ΔR^m, M^m, and R_v^m could be used in D10 for a further correction to the modulation $M^T = M^m - \delta_B M$. However, it is unlikely that these four response factors could be quantified. Besides, the only likely

mechanism for causing K_g' abd K_v' to be other than unity is independent solar solar and reference beam movement on the detectors during an event. In addition, if $K_v' = K_g'$, then from D15 we see that G would be unity and D14 would give $\delta M' = 0$. Therefore, equation D10 should be sufficient for corrections due to instrument response changes.

One final note. It could also be theorized that response changes may occur for only the solar signal. Since this would exhibit no change in AGC, it would be difficult, if not impossible, to detect--much less quantify. However, equations D18, D16, and D14 could be used to make the correction if the response factors were known. Of course, in this case, equation D10 would not apply since no gain change occurs. If these changes were determined to be a function of time from acquisition, correction equations might be deduced from analyzing the data of long duration exoatmospheric tracking events. This idea will be pursued.